

Focal Depths and Mechanisms of Mid-Atlantic Ridge Earthquakes From Body Waveform Inversion

PAUL Y. HUANG, SEAN C. SOLOMON, ERIC A. BERGMAN,
AND JOHN L. NABELEK

Department of Earth, Atmospheric, and Planetary Sciences, Massachusetts Institute of Technology, Cambridge

We have determined the source mechanisms (double-couple orientation, moment, centroid depth, source time function) of 14 earthquakes on the northern Mid-Atlantic Ridge (0° - 72° N) from an inversion of long-period P and SH waveforms. The earthquakes are all characterized by nearly pure normal faulting on fault planes that dip at about 45° and strike parallel to the local trend of the ridge axis. Moments range from 3 to 15×10^{24} dyn cm, and the source time functions are all of simple form. The P and S waveforms for all earthquakes can be well matched using conventional values for t^* (1 and 4 s, respectively). These earthquakes are all very shallow; centroid depths range between 1.2 and 3.1 km beneath the seafloor. The P waves from these earthquakes show strong water column reverberations, suggesting that fault rupture extended to the seafloor. The predominant period of these reverberations constrains the water depth in the epicentral region. On the basis of estimated water depth and epicentral location, all of these earthquakes can be shown to have occurred beneath the inner floor of the median valley. The centroid depths do not show a correlation with either spreading rate or seismic moment. Under the assumption that the centroid depth marks the mean depth of fault slip, earthquake faulting extended to depths of 2-6 km for these events.

INTRODUCTION

Earthquakes along mid-ocean ridges are a primary manifestation of the process of seafloor spreading. Modern study of ridge crest earthquakes dates from the demonstration by Sykes [1967] that such events are characterized by normal faulting mechanisms having T axes that are approximately horizontal and oriented parallel to the direction of spreading. Beyond simple fault plane solutions, relatively few studies have since been made of the source characteristics of ridge crest earthquakes. This is particularly true of focal depth, an extremely important quantity for understanding the depth extent of brittle behavior at ridge crests and its implications for local thermal structure and for such controlling processes as shallow magma injection and cooling by hydrothermal circulation [e.g., Lister, 1977].

While it is generally agreed that ridge crest seismic activity is quite shallow [e.g., Isaacs *et al.*, 1968], well-constrained focal depths have been presented in the literature for only a small number of large ridge crest earthquakes. An early effort to determine the focal depth of ridge crest earthquakes was that of Tsai [1969], who fit Rayleigh wave amplitude spectra from several events to synthetic spectra generated for various source depths and obtained focal depths of 30-65 km. Weidner and Aki [1973] demonstrated, however, that when phase as well as amplitude spectra of Rayleigh waves are considered, the focal depths of ridge crest earthquakes are required to be very shallow; they obtained depths of 3 ± 2 km beneath the seafloor for two normal-faulting events on the axis of the Mid-Atlantic Ridge. Dushenes and Solomon [1977] reported that the short-period P waveforms from these two events contain apparent depth phases consistent with such shallow focal depths. Conventional fault plane solutions derived from P -wave first motions from ridge crest earthquakes often show nonorthogonal nodal planes [Sykes, 1967, 1970; Thatcher and Brune, 1971; Solomon and Julian, 1974], in apparent disagreement with the expected double-couple source model. Hart

[1978] suggested that this nonorthogonality is a consequence of the interference between direct and surface-reflected phases for extremely shallow sources. This suggestion was confirmed by Tréhu *et al.* [1981], who inverted Rayleigh wave spectra for the source moment tensor and synthesized long-period P waveforms for two earthquakes on the Reykjanes Ridge. They showed that both the surface wave spectra and the P waveforms were compatible with double-couple source mechanisms and very shallow focal depths. Pearce [1981] modeled the short-period P waves from a small ($m_b = 4.7$) earthquake on the axis of a spreading center segment in the Gulf of Aden and inferred a focal depth of 5 ± 2 km.

Beyond these few studies of large earthquakes, the remaining published information on the depth of seismogenic faulting along ridge axes comes from microearthquake surveys. While a number of microearthquake studies have been carried out along segments of the Mid-Atlantic Ridge and other ridge systems using either sonobuoys or ocean bottom seismometers, the majority of these experiments were conducted with an insufficient number of stations to resolve focal depths [Dushenes *et al.*, 1983]. Two Mid-Atlantic Ridge microearthquake experiments with networks of more than three instruments are noteworthy exceptions. One was near the eastern intersection of St. Paul's Fracture Zone and the median valley of the ridge [Francis *et al.*, 1978], and the second was within the median valley at a site (near 23° N) distant from major transform faults [Toomey *et al.*, 1985]. Both regions displayed microearthquake activity within the median valley to depths of 7-8 km below the seafloor, and both are also the sites of large earthquakes well recorded at teleseismic distances. These data provide an opportunity to compare the centroid depths of the large earthquakes with the distribution of focal depths of microearthquakes in the same region.

As part of a general and long-term study of earthquakes on mid-ocean ridges and their relationship to the spreading process, we determine in this paper the focal depth and source characteristics of 14 earthquakes along the axis of the Mid-Atlantic Ridge. The source parameters are obtained by a formal inversion of long-period P and SH waveforms. We use the inversion procedure of Nabelek [1984], as applied to

Copyright 1986 by the American Geophysical Union.

Paper number 5B5496.
0148-0227/86/005B-5496\$05.00

TABLE 1. Epicentral Data and Source Parameters for Earthquakes on the Mid-Atlantic Ridge

Date	Origin Time, UT	Latitude °N	Latitude °W	m_b	M_s	M_0 , ^a 10 ²⁴ dyn cm	Mechanism ^b			Centroid Depth, ^c km	Uncertainty in Depth, ^d km	Water Depth, ^e km	Depth of Median Valley, ^f km
							Strike, deg	Slip, deg	Dip, deg				
June 3, 1962	1502:25	22.51	45.08		5.7 ^g	6.1	4	43	274	1.2	1–2	3.9	3.4–4.2
June 2, 1965	2340:23.1	15.93	46.69	5.8	6.0 ^g	8.3	335	38	244	3.0	1–5	3.4	3.5–4.0
Nov. 16, 1965	1524:44.0	31.00	41.53	5.9	6.3 ^g	8.1	25	46	265	2.1	1–3	3.2	3.0–3.5
Sept. 20, 1969	0508:57.8	58.35	32.08	5.6	6.0	15.	23	42	261	1.5	1–3	2.2	1.5–2.0
May 31, 1971	0346:50.6	72.21	–1.09	5.5	5.7	6.8	51	51	284	2.3	2–3	3.1/2.8	2.5–3.0
April 3, 1972	2036:20	54.33	35.20	5.1	5.5	4.4	8	48	254	1.9	1.5–3	2.8	2.0–2.5
June 6, 1972	0525:50.7	32.93	39.79	5.3	5.7	4.1	20	51	253	1.8	1–6	3.2	3.0–3.5
June 28, 1977	1538:37.8	22.64	45.07	5.3	5.6	3.0	1	46	254	2.5	2–9	4.0	3.4–4.2
June 28, 1977	1918:36	22.68	45.11	5.9	6.0	11.	1	44	255	1.6	1–2	3.5	3.4–4.2
Jan. 28, 1979	1945:21	11.92	43.70	5.7	5.6	6.3	20	46	270	2.2	1.5–9	3.7	3.5–4.0
April 22, 1979	0950:13	33.00	39.72	5.6	5.8	9.9	17	52	262	1.8	1.5–2.5	3.3	3.0–3.5
June 28, 1979	0414:44.9	00.40	24.96	5.5	5.2	3.6	346	40	280	2.5	1–4.5	3.5	3.5–4.0
Jan. 29, 1982	2232:06.1	25.52	45.30	5.7	5.8	5.4	9	44	264	2.4	1–4	3.8	3.5–4.0
May 12, 1983	1051:49.7	17.63	46.53	5.7	5.7	7.1	341	48	251	3.1	2–6	4.1	4.0–4.5

Epicentral and magnitude data are taken from the International Seismological Summary for 1962, the ISC for 1964–1982, and the NEIS for 1983.

^aUnits equivalent to 10¹⁷ N m.

^bFocal mechanism specified with the convention of *Aki and Richards* [1980].

^cCentroid depth relative to the seafloor.

^dAt 90% confidence and obtained from the *t* test described in the text.

^eInferred from modeling the water column reverberations in the later portions of the *P* wave trains.

^fLocal maximum depth of the median valley inner floor indicated by bathymetric maps [*Laughton and Monahan*, 1978; *Heezen and Tharp*, 1978; *Johnson et al.*, 1979; *Searle et al.*, 1982; *Toomey et al.*, 1985].

^gMagnitude *M* from *Rothé* [1969].

oceanic intraplate earthquakes by *Bergman et al.* [1984] and *Bergman and Solomon* [1984, 1985a]. Because of the special importance of focal depth, we devote particular attention to the resolution of centroid depth and to an assessment of the relationship between the formal error given by the inversion method and actual uncertainty. After a presentation of the results of individual inversions, we generalize to a discussion of the implications of the derived source parameters for median valley tectonics along slow spreading ridge systems.

EARTHQUAKE DATA SET

We began our study with a search for earthquakes on the Mid-Atlantic Ridge large enough to yield clear long-period *P* and *S* waves at teleseismic distances and having an epicenter within the median valley of an active ridge segment. The search included the catalog of *Rothé* [1969] for 1962–1965, the bulletins of the International Seismological Centre (ISC) for the years 1964–1982, the monthly listings of the National Earthquake Information Service (NEIS) for the years 1982–1983, and published studies of fault plane solutions for Mid-Atlantic Ridge earthquakes [*Sykes*, 1967, 1970; *Solomon and Julian*, 1974; *Udias et al.*, 1976; *Einarsson*, 1979; *Savostin and Karasik*, 1981; *Dziewonski et al.*, 1983a, b]. Particular care was taken to exclude near-ridge intraplate events [*Bergman and Solomon*, 1984]. We restricted the search to the northern Mid-Atlantic Ridge, between latitudes 0° and 80°N, primarily to ensure a good azimuthal distribution of teleseismic stations. Earthquakes on the Arctic Ridge system are treated separately in a parallel study [*Jemsek et al.*, 1984].

The 14 selected earthquakes are listed in Table 1; their epicenters are shown in Figure 1. For all of the events in the table, we have found at least 10 clear *P* and *SH* waves recorded on long-period instruments at stations of the World-Wide Standard Seismograph Network (WWSSN) or the Global Digital Seismic Network (GDSN) at epicentral distances between 30° and 80°. The events range between latitudes 0.4° and 72.2°N and have epicenters within median valley segments on bathymetric maps of the “General Bathymetric Chart of the

Oceans” (GEBCO) series [*Laughton and Monahan*, 1978; *Heezen and Tharp*, 1978; *Johnson et al.*, 1979; *Searle et al.*, 1982]. The local half-spreading rates vary from 0.8 to 1.8 mm/yr according to the plate kinematic model of *Minster and Jordan* [1978]. The earthquakes have body wave magnitude m_b between 5.1 and 5.9, and as demonstrated below, all have focal mechanisms characterized by normal faulting. We believe that this list is exhaustive, given our selection criteria, for the period 1962 to mid-1983.

WAVEFORM INVERSION PROCEDURE

For each of the 14 earthquakes in this study, we determined the best fitting double-couple point source from an inversion of long-period *P* and *SH* waveforms recorded by WWSSN stations at epicentral distances between 30° and 80°. We employed the inversion technique of *Nabelek* [1984] as applied by *Bergman et al.* [1984]. The inversion yields centroid depth and source time function as well as double-couple orientation and seismic moment. The orientation of the best fitting double couple is determined to within about ±5° formal error in each angular coordinate, and the moment to within about ±30%, at the 2σ (95% confidence) level. The formal error (2σ) in centroid depth is typically ±0.1 to 0.3 km, but because of bias introduced by factors not reflected in the estimate of a posteriori parameter variances, such as the alignment in time between the synthetic and observed waveforms, the true uncertainty may be greater, perhaps ±2 km in some cases. A detailed investigation of the depth resolution for ridge axis events is discussed below. Resolution of all source parameters may be degraded, of course, by such factors as poor station distribution, poor signal-to-noise ratio, or source complexity.

All inversions were performed with the same source velocity structure: a water layer with thickness estimated from bathymetric maps, a single crustal layer of thickness 6 km and *P* and *S* wave velocities $\alpha = 6.4$ km/s and $\beta = 3.7$ km/s, respectively, and a mantle half-space with $\alpha = 8.1$ km/s and $\beta = 4.6$ km/s. Further constraint on the water depth is provided by

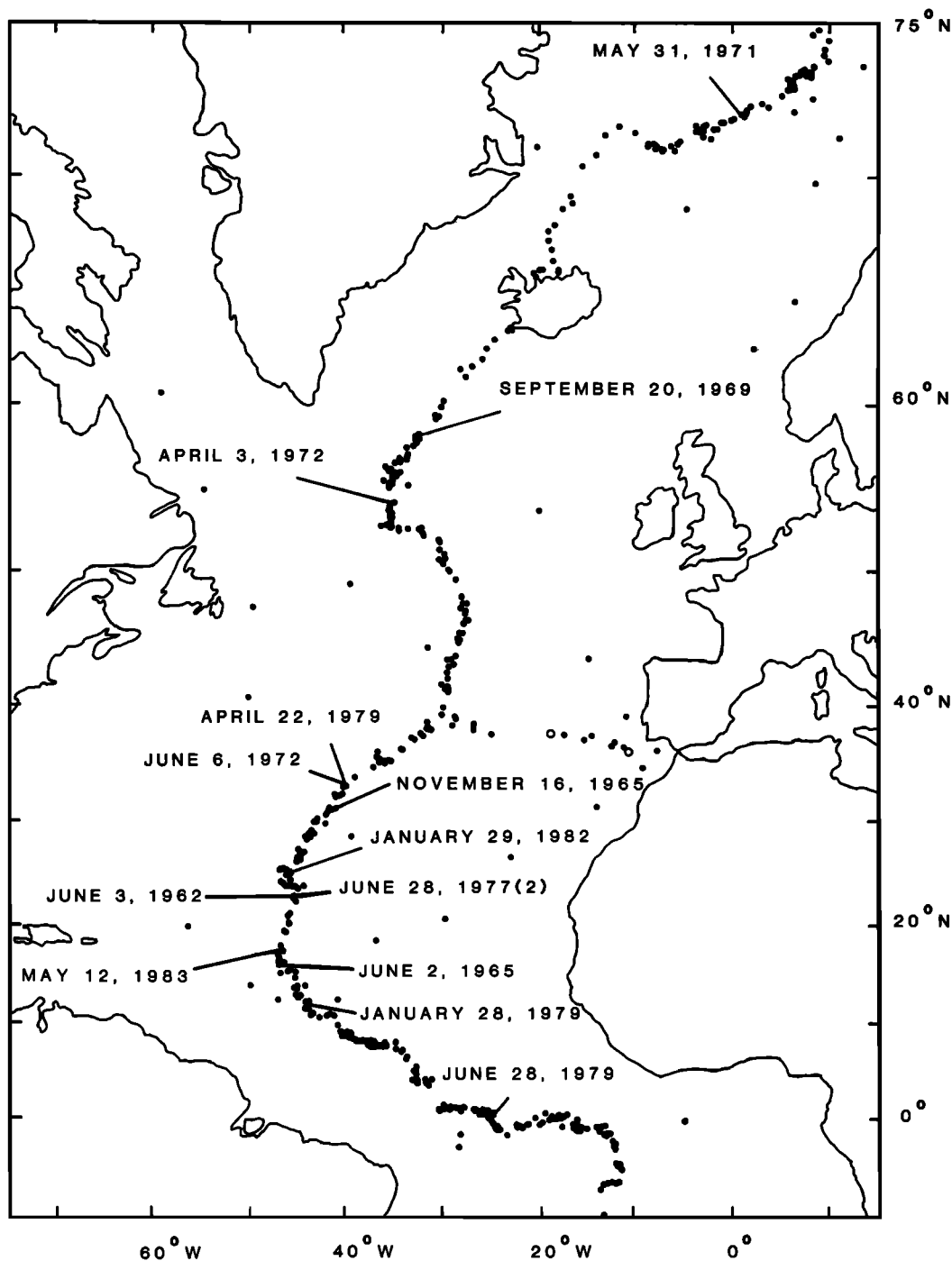


Fig. 1. Location of Mid-Atlantic Ridge earthquakes studied in this paper, along with the overall distribution of seismicity [Tarr, 1974]. Solid circles show earthquakes with $m_b \geq 4.5$ during 1963–1972; open circles denote events in this century with $M_s \geq 8$.

the predominant period of water column reverberations, seen as prominent phases immediately following the P wave arrival. A crustal thickness of about 6 km has been reported for several axial valley segments along the Mid-Atlantic Ridge [Fowler, 1976; Bunch and Kennett, 1980; Purdy and Detrick, 1986]. While uniform velocity crust and mantle layers are an oversimplification of the actual structure, we demonstrate below that the waveform inversion results are generally insensitive to details of source structure. To the extent that the seismic velocities in the uppermost crust are less than assumed in the uniform layer model, the actual centroid depths may be somewhat shallower than the values derived from the inversions.

Other aspects of data reduction and waveform synthesis follow the procedure of Bergman *et al.* [1984]. In particular, we employed the conventional values of 1.0 and 4.0 s for the attenuation parameter t^* [Futterman, 1962] for long-period P and SH waves, respectively. Because there is significant trade-off between t^* and source time function, more precise values of t^* cannot be independently determined from our inversion.

DEPTH RESOLUTION

Since the centroid depths found for ridge axis events are perhaps the most important new source parameters reported here, the depth resolution of our inversion procedure deserves particular attention. For a variety of reasons, as noted above,

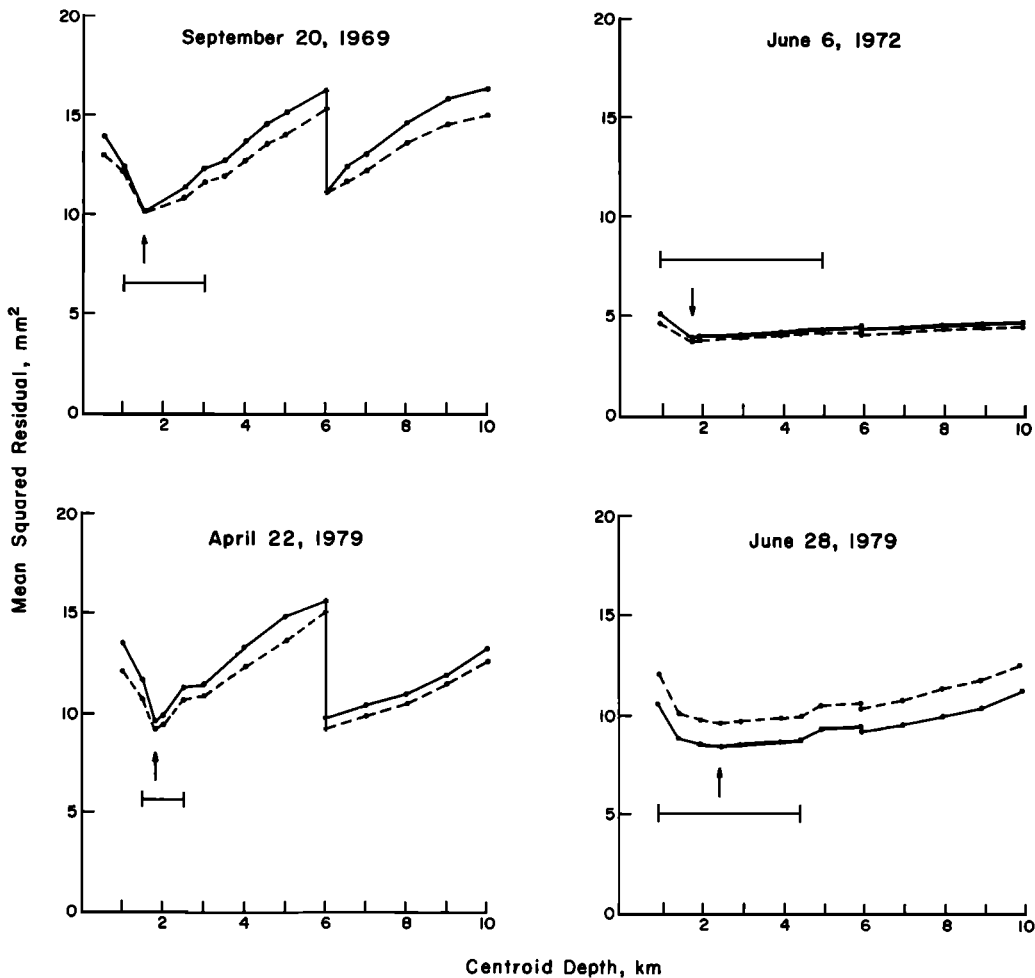


Fig. 2. Mean squared residual versus centroid depth for four earthquakes in this study. The solid and dashed lines indicate residuals r^2 and R^2 , defined in equations (1) and (3), respectively. The horizontal bar indicates the 90% confidence interval about the best fitting depth found in the body waveform inversion, which is indicated by an arrow.

the formal uncertainty calculated in the inversion may underestimate the depth resolution actually achievable. The parameters of the best fitting point source are those which minimize the mean square residual r^2 , defined as

$$r^2 = \frac{\sum_{j=1}^N \sum_{i=1}^{M_j} w_j (s_{ij} - o_{ij})^2}{\sum_{j=1}^N M_j} \quad (1)$$

where s_{ij} and o_{ij} are the amplitudes of the synthetic and observed seismograms at station j and time sample i , w_j is the weight used for station j , M_j is the number of samples in the time window used in the inversion for station j , and N is the total number of stations. A station with both a P and an SH waveform used in the inversion is counted twice in (1). The station weights w_j are in inverse proportion to the noise level prior to the start of the time window.

As a first step in an investigation of the depth resolution of the inversion, we fixed the centroid depth at a range of values and inverted for the remaining source parameters to minimize r^2 . At each depth, we realigned the synthetic and observed waveforms as necessary to improve the overall fit. This procedure is analogous to the one commonly used (in the frequency domain) to estimate earthquake source depths from surface wave amplitude and phase spectra [e.g., Weidner and Aki, 1973; Aki and Patton, 1978; Romanowicz, 1981, 1982].

For all of the events in this study, we found that the mean square residual versus depth displayed two minima, one located in the crust and one just below the crust-mantle interface (Figure 2). The question of depth resolution therefore involves two separate issues. The first concerns the choice between the two minima in the relation for residual versus depth. The second issue is the estimation of uncertainty in the depth at which the preferred minimum occurs.

Without exception, the solution within the crust has a smaller residual than the sub-Moho solution and would therefore be the preferred solution. The difference in residuals (Figure 2) is small, however, and the other source parameters are similar for both depths. Because the deeper solution usually lies immediately below the crust-mantle interface in the adopted source velocity structure, we suspect that it is an artifact of the assumed sharp velocity contrast. To investigate this possibility, we performed inversions of waveforms from the September 20, 1969, Reykjanes Ridge earthquake using a variety of crustal models. Our first series of tests examined the effect of different crustal thicknesses on the depths and relative magnitude of the two minima in r^2 . For a half-space model with crustal P and S velocities there is only one minimum, at 1.4 km below the seafloor. When a crustal layer greater than 1.5 km in thickness is assumed for the source structure, a stable minimum in r^2 develops at about 1.5 km depth, and the second minimum appears immediately below the crust-mantle interface. With a progressively thicker crustal layer this second

minimum moves with the layer boundary, suggesting that the sharp velocity contrast at the Moho acts to reflect energy downward in a manner similar to the water-crust boundary. To test this hypothesis, we repeated the inversions with a velocity model which has an additional layer in the lower crust to simulate a gradual increase in velocity across the crust-mantle transition. The sub-Moho solution becomes severely degraded as the velocity contrast at the Moho proper is reduced. It is quite probable that our simple source crustal structure overestimates the velocity contrast at the Moho beneath a slowly spreading ridge [e.g., Purdy and Detrick, 1986]. We conclude from these results that the shallow crustal solution is stable for any reasonable crustal thickness and that it probably represents the true solution for these earthquakes.

Other source parameters were consistent for all of the different structural models we have tested, including the model with no crustal layer and the model with two crustal layers. The seismic moment varied by less than 20%, strike and dip varied by less than 10°, and slip varied by less than 20°. We conclude from this exercise that the results of long-period waveform inversion are largely insensitive to the details of the velocity structure.

To investigate the uncertainty in the depth of the crustal level minimum in r^2 , we conducted a test of significance for the differences in station residuals between waveforms for the best fitting depth and those obtained when the inversion is performed with the depth fixed at nearby values. By using the residuals at individual stations as our data instead of the residual at each discrete time sample, we are assured of independent data. This approach underestimates the number of degrees of freedom, however, and will yield a very conservative result. The mean square residual for station j is

$$r_j^2 = \frac{1}{M_j} \sum_{i=1}^{M_j} (s_{ij} - o_{ij})^2 \quad (2)$$

We also redefine the mean square residual for the model as

$$R^2 = \frac{1}{N} \sum_{j=1}^N r_j^2 \quad (3)$$

The quantities r^2 and R^2 in (1) and (3) would be equal only if all stations have the same inversion window length and weight. We investigated the distribution of individual station residuals r_j^2 with the χ^2 test for goodness of fit and found that the residuals can generally be considered to follow a normal distribution.

We now consider the matched station residuals at two depths A and B and the set of differences

$$d_j = r_{jA}^2 - r_{jB}^2 \quad j = 1, 2, \dots, N$$

We denote the mean and standard deviation of the set of d_j by μ_d and σ_d , respectively. The set of d_j may be regarded as sampling a normally distributed population of station residual differences with mean μ_D and standard deviation σ_D . We test the null hypothesis $\mu_D = 0$ by forming the statistic

$$t = \frac{\mu_d}{\sigma_d/(N)^{1/2}}$$

which follows the t distribution with $N - 1$ degrees of freedom. Since we are testing the hypothesis that the solution at one depth is better than the other, we use the one-tailed (or one-sided) test.

We investigated the depth resolution of the inversion by considering the differences between residuals at the best fitting

depth and those at nearby depths, both shallower and deeper. Specifically, we determined the depths at which the t statistic exceeds the allowed value for a significance level of 0.1. The depth ranges determined in this manner for four ridge axis earthquakes are shown in Figure 2, along with the mean square residuals r^2 and R^2 as functions of source depth. The depth ranges indicated by the t test for all 14 earthquakes are given in Table 1. In general, the resolution of the centroid depth estimated by the t test is consistent with a formal error of about $10\sigma_h$, where σ_h is the standard error in the centroid depth h determined in the waveform inversion.

The range in uncertainty about the best fitting depth is not symmetric; it is smaller (averaging -1.0 km for the 14 events in Table 1) at the shallow end than at the deeper end (averaging $+2.3$ km). The uncertainty range tends to be smaller for larger earthquakes, probably because more stations are used for larger events, thus the source mechanism is better constrained. It should be recalled that we have underestimated the number of degrees of freedom for all these tests in order to be assured of independent data.

Finally, it should be noted that statistical considerations are not the sole basis for drawing inferences; a physical appreciation of the problem and experience may also be brought profitably into the judgment. To illustrate how details of waveform shapes which are poorly reflected in the mean square residual can be important clues in judging the success of a particular solution, we have plotted in Figure 3 the observed and synthetic P waveforms at three stations generated with the best fitting source parameters at five depths for the earthquake of June 6, 1972. For this earthquake, the plot of mean squared residual versus centroid depth (Figure 2) is very flat at depths greater than about 1.5 km, and the range of statistical uncertainty is large. On this basis alone, we would conclude that long-period waveform data place virtually no constraint on the depth of this event. On the other hand, the character of the first half-cycle of motion of the synthetic P waveforms in Figure 3 allows us to distinguish a centroid depth of 1.8 km as being superior to solutions even 1 km shallower or deeper. The solution at a depth of 1 km does not produce a large enough dilatation at CAR. The solution at 3 km produces too large a dilatation at AAE and AQU, and the width of the first pulse at CAR is too wide. The solutions at 4 and 5 km progressively aggravate these problems, although the overall residual error remains nearly constant. We conclude that the range in acceptable centroid depths determined in the statistical study is a good, although rather conservative, estimate of the true uncertainty in the depth estimated in the inversion.

WAVEFORM INVERSION RESULTS

In this section, we present the source parameters obtained from the inversion of P and SH waveforms for the 14 ridge axis earthquakes. The best fitting double-couple orientation, seismic moment, and centroid depth are given in Table 1. The convention for describing double-couple orientation is that of Aki and Richards [1980]. Centroid depths are given relative to the top of the crust. Also listed in Table 1 is the average water depth above each hypocenter obtained by matching the synthetic and observed seismograms in the ringing portion of the P wave train.

June 3, 1962

The earthquake of June 3, 1962, occurred in the Mid-Atlantic Ridge median valley about 100 km south of the Kane Fracture Zone (Figure 4). Because this event predates the es-

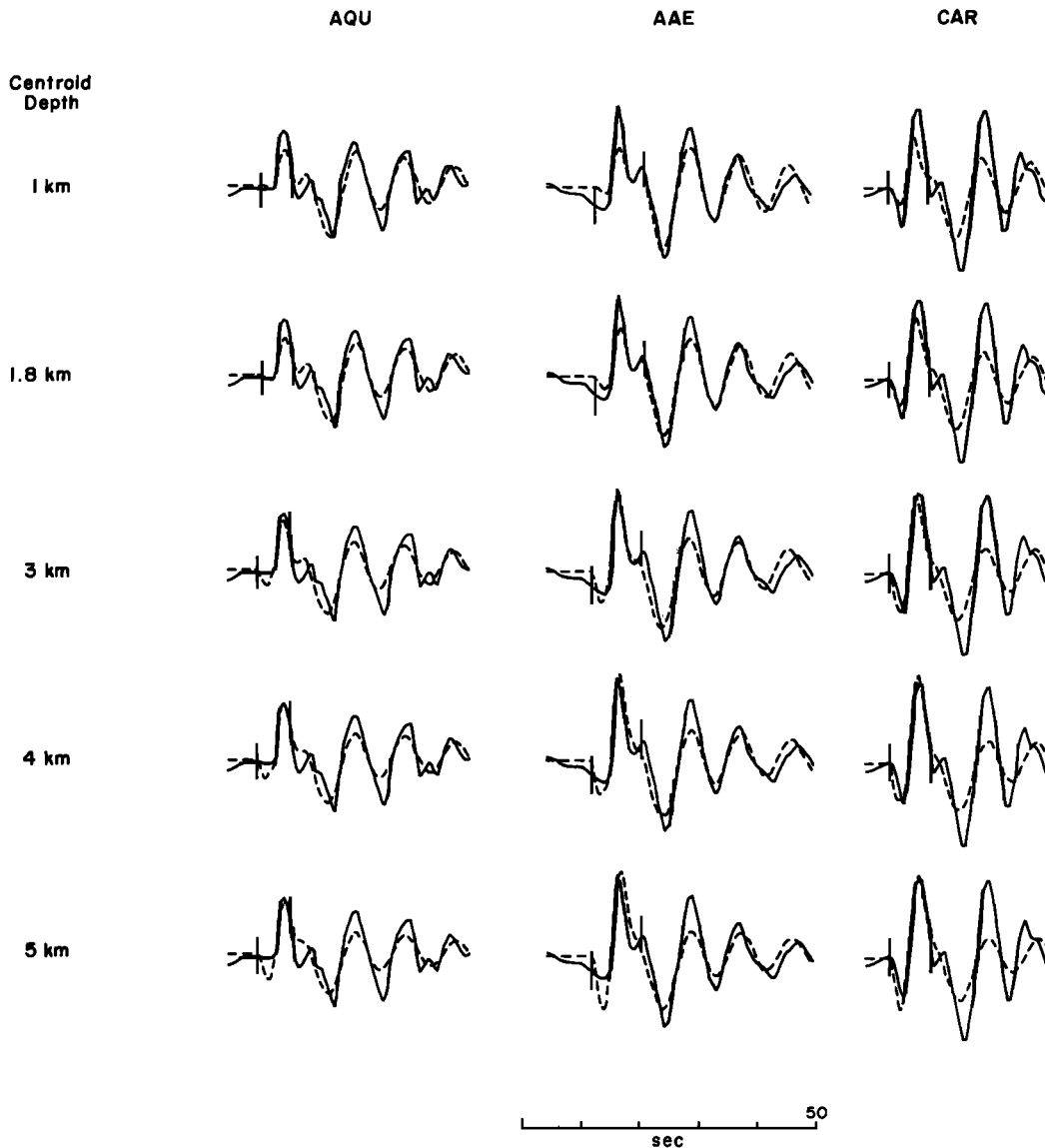


Fig. 3. Comparison of observed (solid) and synthetic (dashed) P waveforms at three stations for the earthquake of June 6, 1972. The synthetic seismograms are generated from the best fitting solution obtained with the centroid depth fixed at the value indicated. Additional waveforms not shown (see Figure 15) are used in the inversions. The preferred centroid depth is 1.8 km. Vertical tic marks delimit the portions of the waveforms included in the inversions.

establishment of many WWSSN stations, station coverage is rather poor, and resolution of the focal mechanism is less than ideal. The inversion solution (4/43/274) (strike/slip/dip) represents nearly pure dip-slip motion (Figure 5) with a seismic moment of 6.1×10^{24} dyn cm. The centroid depth of 1.2 km is quite well constrained (Table 1). The 3.9-km water depth estimated from the predominant period of water reverberations in the P waveforms is slightly greater than the depth of the median valley inner floor at the nominal latitude of the epicenter.

June 2, 1965

The June 2, 1965, earthquake, which occurred in the median valley about 50 km north of the 15°20' Fracture Zone (Figure 6), has been the subject of several previous studies. On the basis of P wave first-motion polarities, Sykes [1970] found a normal faulting mechanism with nonorthogonal nodal planes. Tsai [1969] estimated the seismic moment to be 2.8×10^{25} dyn cm from the Rayleigh wave amplitude spectrum at one

station, but this value was based on an adopted focal depth of 65 km. Using both the amplitude and phase spectra of Rayleigh waves from a number of stations, Weidner and Aki [1973] demonstrated that the focus is actually quite shallow (3 ± 2 km). They also obtained a best fitting double couple (0/40/260) and a seismic moment of 7.8×10^{24} dyn cm. From the identification of pP on short-period P waveforms, Duchenues and Solomon [1977] estimated a focal depth of 2 ± 1 km.

The body wave inversion solution (335/38/244) is shown in Figure 7. The SH waves provide exceptional coverage, and all the observed waveforms are well fit. The westward dipping nodal plane has a strike slightly east of north, parallel to the local trend of the ridge axis. A small component of strike-slip motion is required in order to fit the SH waveforms to the northeast, particularly GDH and KTG, where the small dilatation of the direct SH phase is clearly seen. The best fitting seismic moment is 8.3×10^{24} dyn cm, and the centroid depth is 3.0 km. Both values agree quite well with those of Weidner

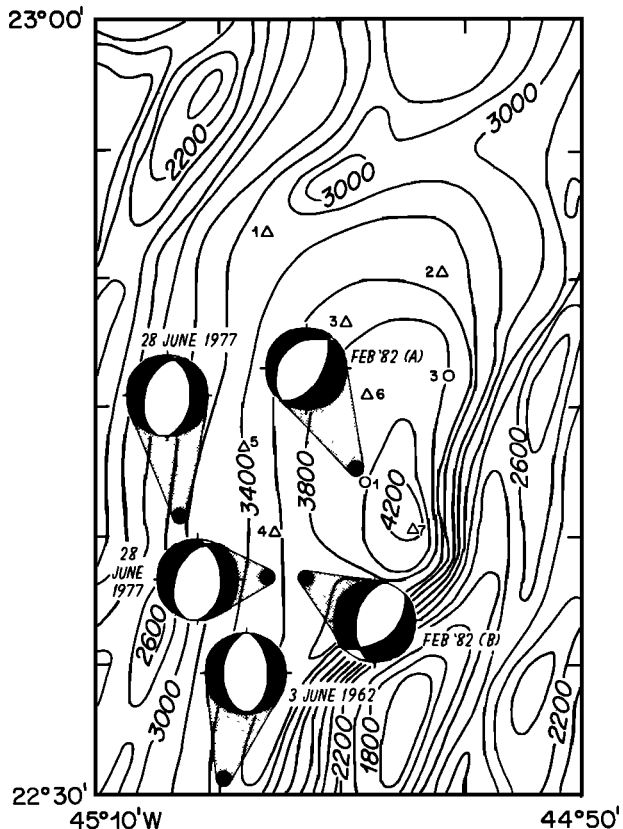


Fig. 4. Detailed bathymetry of the Mid-Atlantic Ridge median valley near the epicenters of the earthquakes of June 3, 1962, and June 28, 1977. Bathymetric contours, in meters, are from Toomey *et al.* [1985]. The location of this region relative to neighboring elements of the Mid-Atlantic Ridge system is shown in Figure 22. Fault plane solutions are equal-area projections of the lower focal hemisphere; compressional quadrants are shaded. Mechanisms labeled A and B for February 1982 are composite fault plane solutions determined by Toomey *et al.* [1985] for two clusters of microearthquakes recorded by a network of ocean bottom seismometers and ocean bottom hydrophones located at the positions shown by numbered circles and triangles, respectively.

and Aki [1973]. The water depth inferred from the *P* waveforms is 3.4 km.

November 16, 1965

The earthquake of November 16, 1965, occurred in the median valley about 100 km north of the Atlantis Fracture Zone (Figure 8). From *P* wave first motions, Sykes [1967] found a normal faulting mechanism with nonorthogonal nodal planes. Tsai [1969] estimated the seismic moment to be 5.2×10^{25} dyn cm from the Rayleigh wave amplitude spectrum at one station, based on an assumed focal depth of 45 km. Weidner and Aki [1973] estimated a focal depth of 3 ± 2 km using both amplitude and phase spectra of Rayleigh waves. They also reported a best fitting double couple of 0/59/234 and a seismic moment of 1.2×10^{25} dyn cm. From an identification of the short-period *pP* phase, Dushenes and Solomon [1977] obtained a focal depth of 4 ± 2 km.

The inversion solution (Figure 9) shows nearly pure normal faulting (25/46/265) on a fault plane whose strike is much closer to the trend of the ridge axis than the mechanism of Weidner and Aki [1973]. The distribution of *P* and *SH* waves provides a good sampling of the focal spheres. In particular, the nodal *SH* waveforms at MDS and LPB constrain the strike of the double couple. The seismic moment is 8.1×10^{24}

dyn cm, the centroid depth is 2.1 km and is well constrained (Table 1), and the inferred water depth is 3.2 km.

September 20, 1969

The September 20, 1969, earthquake occurred on the Reykjanes Ridge (Figure 10), about 100 km south of a transition in the character both of ridge axis seismicity and axial valley morphology [Francis, 1973; Vogt and Johnson, 1975]. To the north of about 59°N the ridge is anomalously shallow, lacks a prominent median valley, and is nearly aseismic, presumably a result of the influence of the Iceland hot spot; to the south of 59°N the seismicity and median valley morphology are more typical of other sections of the Mid-Atlantic Ridge. Using *P* wave first-motion data, Solomon and Julian [1974] obtained a normal-faulting mechanism with nonorthogonal nodal planes. They showed that if the projection of first-motion data onto the focal sphere were corrected for propagation through a laterally heterogeneous model of the velocity structure beneath the ridge axis, a focal mechanism with orthogonal nodal planes could be found (9/41/263). Hart [1978] modeled the *P* waveforms from this earthquake as a forward problem. He argued that with a shallow focal depth (2.1 ± 0.2 km) the waveforms, including those with apparently anomalous first motions, can be matched with a double-couple source (9/35/260). He obtained a moment of 2×10^{25} dyn cm.

The observed *P* and *SH* waves show good signal-to-noise ratio and are well distributed, so the waveform inversion problem is unusually well constrained (Figure 11). The E-W component at NAT and both horizontal components at NIL were found to have reversed polarity and were corrected prior to inversion. The inversion solution (23/42/261) differs slightly in strike from that reported by Hart [1978], but the *P* waveforms alone allow only loose constraints to be placed on the fault strike; the *P* waveforms in Figure 11 are exceptionally well fit by the synthetic seismograms. We obtained a moment of 1.5×10^{25} dyn cm and a centroid depth of 1.5 km, both slightly smaller than the values reported by Hart [1978]. The 90% confidence interval for centroid depth as given by the *t* test is 1–3 km (Figure 2). The indicated water depth is 2.2 km, consistent with an epicenter in the central median valley of this shallow ridge system (Figure 10).

May 31, 1971

The May 31, 1971, earthquake occurred north of Iceland on the Mohs Ridge (Figure 12). Conant [1972] obtained a normal faulting mechanism with nonorthogonal nodal planes from *P* wave first motions. Savostin and Karasik [1981] used a larger data set to constrain the focal mechanism to a combination of normal and strike-slip faulting (141/59/220). Such a mechanism, however, does not fit the observed *P* and *SH* waveforms. From waveform inversion we obtained a normal-faulting mechanism (Figure 13) with only a small strike-slip component (51/51/284). We have excellent azimuthal coverage for both *P* and *SH* waves, and most observed waveforms are well fit. The seismic moment is 6.8×10^{24} dyn cm, and the focal depth is 2.3 km and well constrained (Table 1).

Two slightly different water depths were indicated by the water column reverberations in the *P* wave trains. Stations to the east (SHL, KBL, MSH, IST, AQU, and TOL) are consistent with a water depth of 3.1 km, while stations to the west (TRN, WES, AAM, DUG, and COL) suggest a somewhat shallower water depth of 2.8 km. We interpret this pattern as indicating an epicenter near the northwestern wall of the median valley inner floor, a location about 15 km north or northwest of the ISC epicenter (Figure 12).

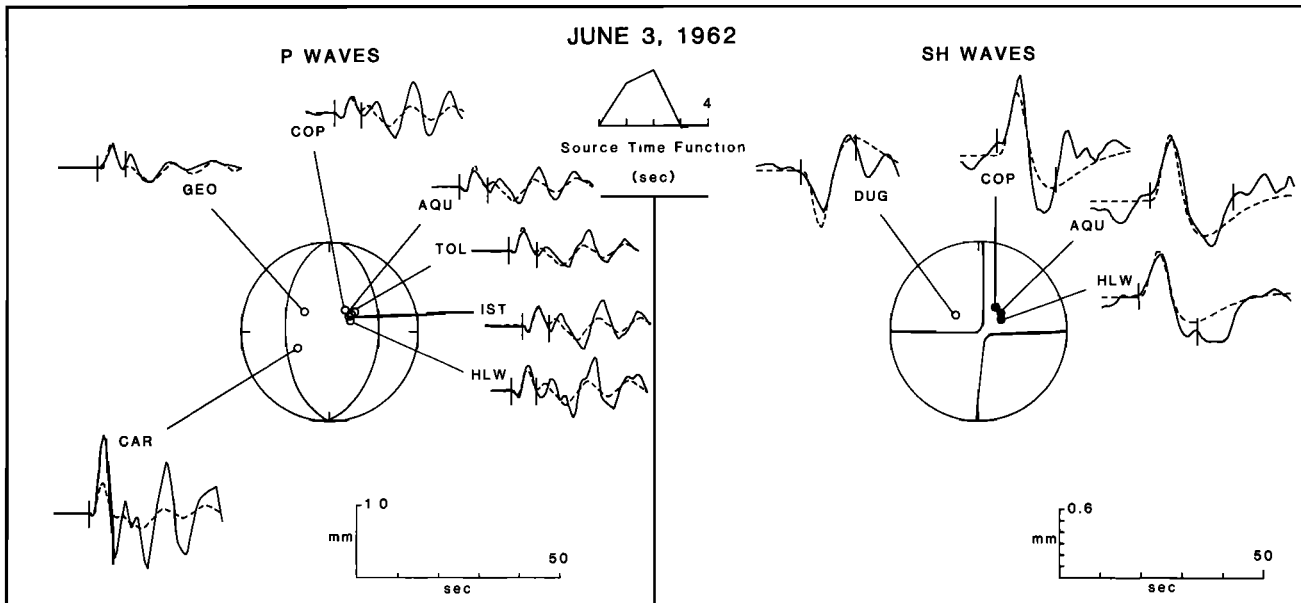


Fig. 5. Comparison of observed (solid line) and synthetic (dashed line) long-period P and SH waves for the June 3, 1962, earthquake, with the focal mechanism solution obtained from the inversion plotted on the lower focal hemisphere (equal-area projection). All amplitudes are normalized to an instrument magnification of 3000; the amplitude scales correspond to the waveforms that would be observed on an original seismogram from such an instrument. The two vertical lines delimit the portion of each time series, digitized at 0.5-s intervals, used in the inversion. Symbols for both types of waves are open circle, dilatation; solid circle, compression; cross, emergent arrival. For SH waves, compression corresponds to positive motion as defined by Aki and Richards [1980]. Some first motions are shown for stations not used in the waveform inversion. The source time function obtained from the inversion is also shown.

April 3, 1972

The April 3, 1972, earthquake occurred on the southern Reykjanes Ridge, about 150 km north of its intersection with the Gibbs Fracture Zone (Figure 10). Einarsson [1979] obtained a normal-faulting mechanism with nonorthogonal nodal planes from P wave first motions. From a moment tensor inversion of the Rayleigh wave radiation pattern and forward modeling of long-period P waveforms, Tréhu *et al.* [1981] found a pure normal faulting mechanism (4/46/270) and suggested that the apparent nonorthogonality is due to the shallowness of the source. They matched the P waveforms with a finite source of length 13 km, width 3 km, and moment 7.5×10^{24} dyn cm, with rupture initiating near the center of the fault and extending to the seafloor. The focal mechanism of Tréhu *et al.* [1981] provides a good match to the P waveforms, but there are significant discrepancies with the SH waveforms at AAE, JER, and TUC. The inversion solution (8/48/254) has slightly more strike-slip motion (Figure 14) and matches all P and SH waveforms. The centroid depth of 1.9 km obtained from the inversion is somewhat deeper than the 1.1 km indicated by the finite fault model of Tréhu *et al.* [1981]. The seismic moment of 4.4×10^{24} dyn cm given by the body waveform inversion is smaller than that obtained by Tréhu *et al.* [1981] from the forward modeling of P waveforms and from the moment tensor inversion of Rayleigh waves. The inferred water depth of 2.8 km is consistent with an epicenter in a locally deep portion of the median valley inner floor (Figure 10).

June 6, 1972

The June 6, 1972, earthquake occurred in the Mid-Atlantic Ridge median valley about 100 km south of the Hayes Fracture Zone (Figure 8). Station coverage for both P and SH waves is mostly confined to the northern hemisphere. The

inversion solution (20/51/253) represents predominantly normal faulting (Figure 15) with a small strike-slip component. The strike of the fault planes is constrained by the SH waves at KTG, KEV, and CAR. The seismic moment is 4.1×10^{24} dyn cm, the centroid depth is 1.8 km (Figure 3), and the indicated water depth is 3.2 km.

June 28, 1977

On June 28, 1977, an earthquake swarm occurred near the epicenter of the June 3, 1962, earthquake discussed above (Figure 4). The ISC lists five events over a 4-hour period. The first in the series (1538:37.8) had $m_b = 5.3$, $M_s = 5.6$; the fourth and largest in the series (1918:36) had $m_b = 5.9$, $M_s = 6.0$.

The inversion solution for the largest earthquake of the swarm (Figure 16) represents nearly pure normal faulting (1/44/255), a solution very similar to that of the June 3, 1962, earthquake. Although the SH wave coverage is confined to the northern hemisphere, several SH waveforms strongly constrain the focal mechanism. The seismic moment is 1.1×10^{25} dyn cm, and the centroid depth is 1.6 km. The inferred water depth is 3.5 km, indicating that the ISC epicenter is mislocated by 6–7 km to the west (Figure 4).

The inversion solution for the first swarm event (Figure 17) is also characterized by normal faulting with only a small strike-slip component (1/46/254), nearly identical to that of the larger event. The seismic moment is 3.0×10^{24} dyn cm, and the centroid depth is 2.5 km, somewhat deeper than the later, larger event in the series. The inferred water depth is 4.0 km, greater than that of the larger event but also consistent with an epicenter in the central median valley about 10 km east of the ISC location (Figure 4). Because all of the stations for this event are located in the northern hemisphere, the inversion solution is not well constrained. In particular, a solution with a larger strike-slip component (355/50/241) and a greater cen-

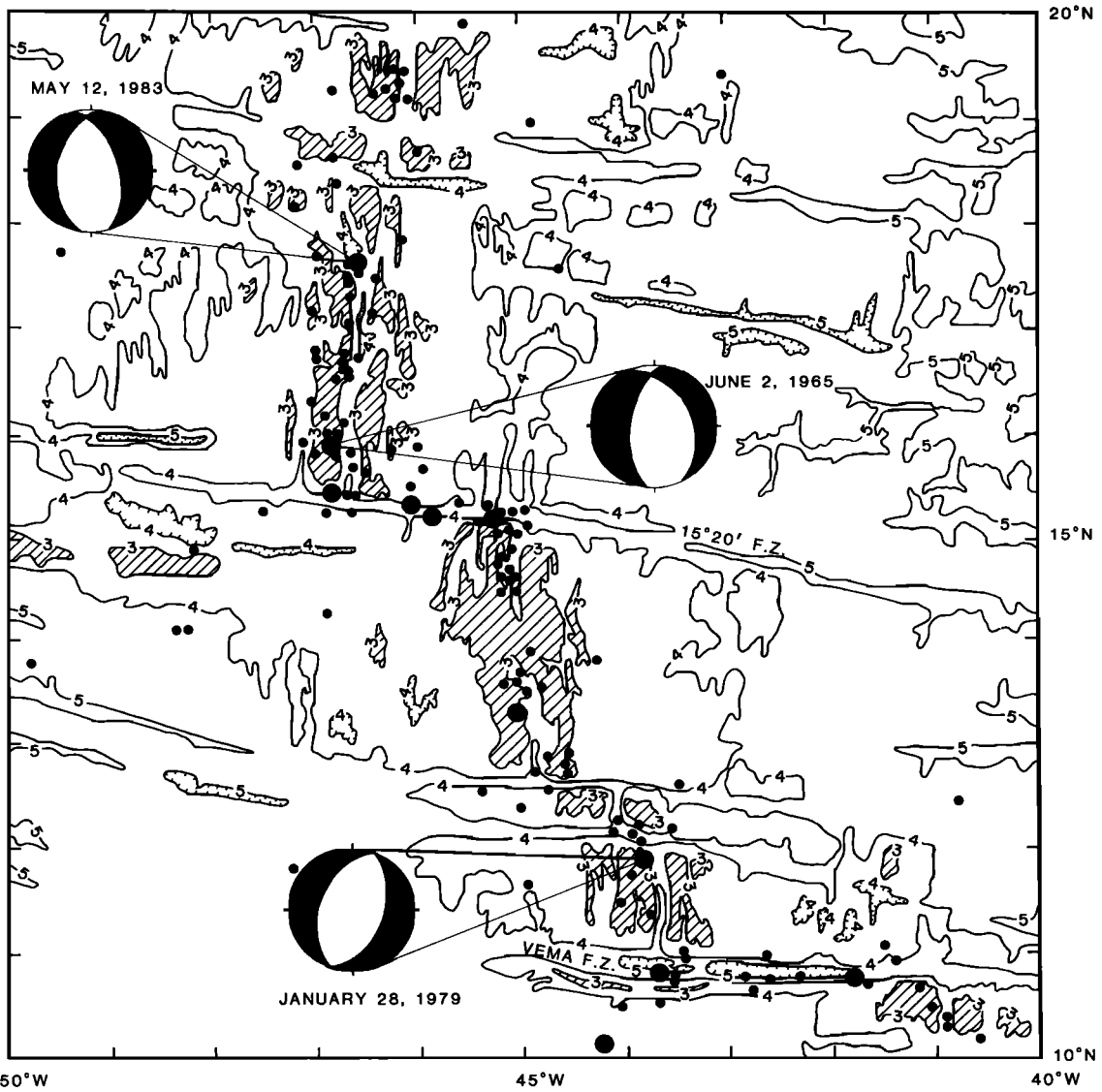


Fig. 6. Bathymetry and seismicity of the Mid-Atlantic Ridge near the epicenters of the earthquakes of June 2, 1965; January 28, 1979; and May 12, 1983 (Mercator projection). Bathymetric contours, in kilometers, are from Searle *et al.* [1982]; regions shallower than 3 km are shaded. Earthquake epicenters are from the ISC for 1964-1979; larger symbols denote events with $m_b \geq 5.4$. Fault plane solutions for events of this study are equal-area projections of the lower focal hemisphere; compressional quadrants are shaded.

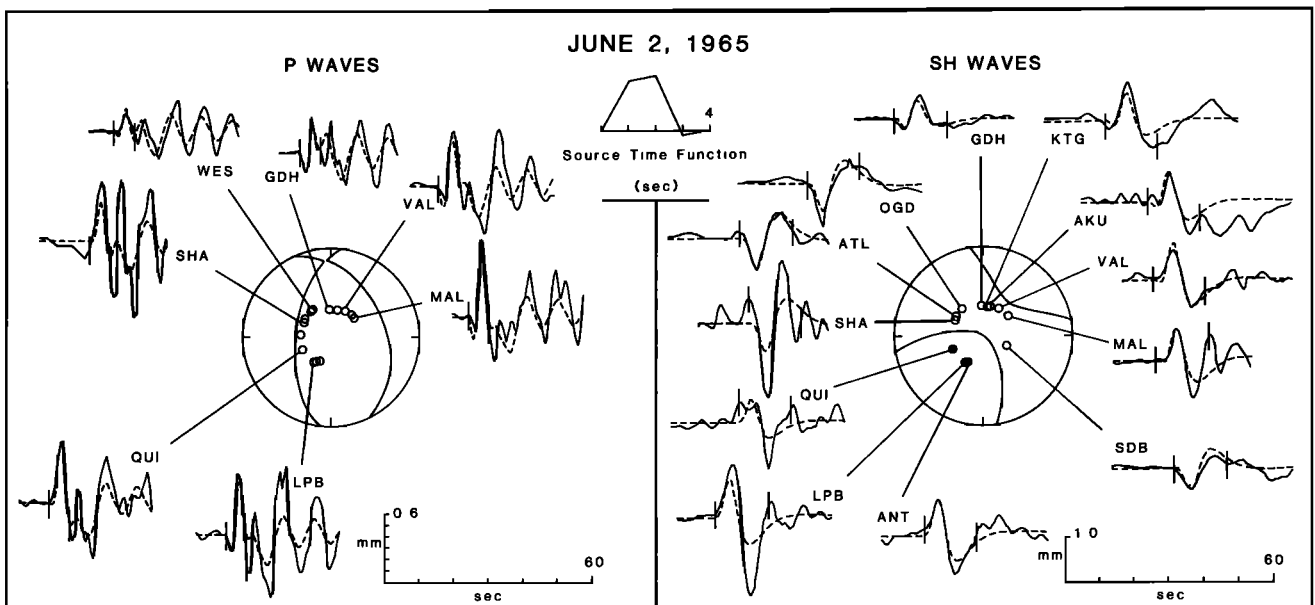


Fig. 7. Comparison of the observed and synthetic P and SH waves for the June 2, 1965, event. See Figure 5 for further explanation.

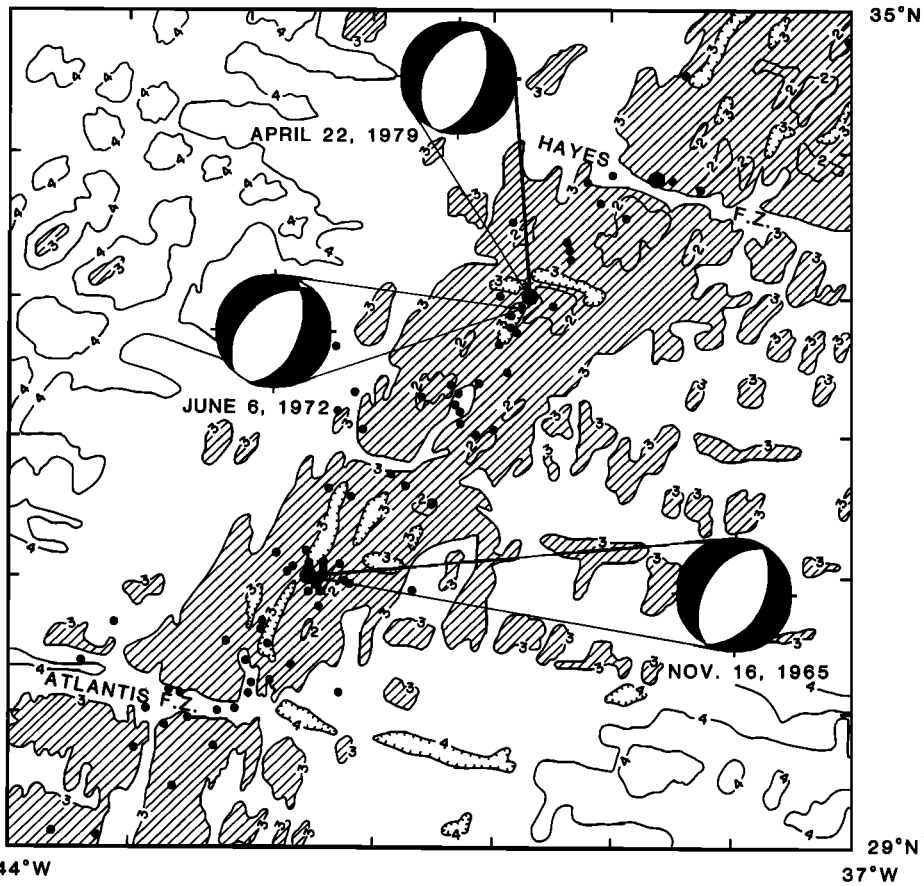


Fig. 8. Bathymetry and seismicity of the Mid-Atlantic Ridge near the epicenters of the earthquakes of November 16, 1965; June 6, 1972; and April 22, 1979. Bathymetry is from Searle *et al.* [1982]; see Figure 6 for further explanation.

troid depth (5.5 km) fits the observed waveforms about as well as the shallow solution. We prefer the shallow solution because its mechanism is similar to those of other large earthquakes (with better station coverage) and of microearthquakes in this area (Figure 4). A preliminary analysis of short-period

body waveforms from this event also indicates that the shallow solution is preferable [Bergman and Solomon, 1985b].

The *P* waveforms of another event in this swarm (1618:16, $m_b = 5.5$, $M_s = 5.7$) are obscured by the surface waves from the earthquake 40 min before. A normal faulting mechanism

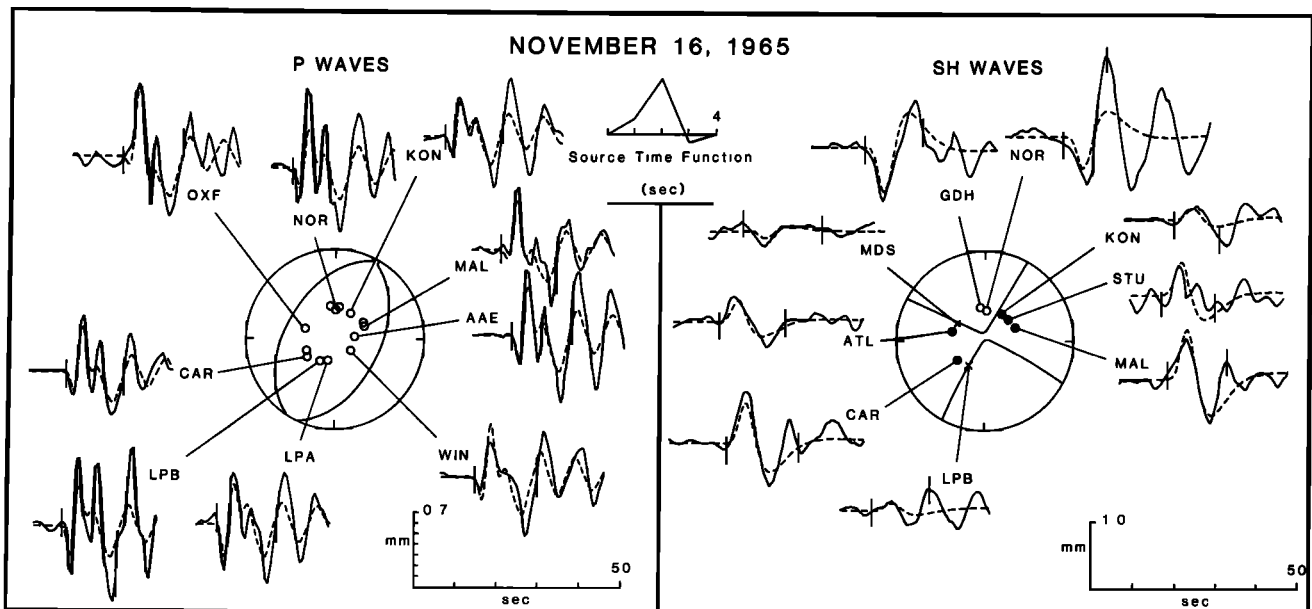


Fig. 9. Comparison of the observed and synthetic *P* and *SH* waves for the November 16, 1965, event. See Figure 5 for further explanation.

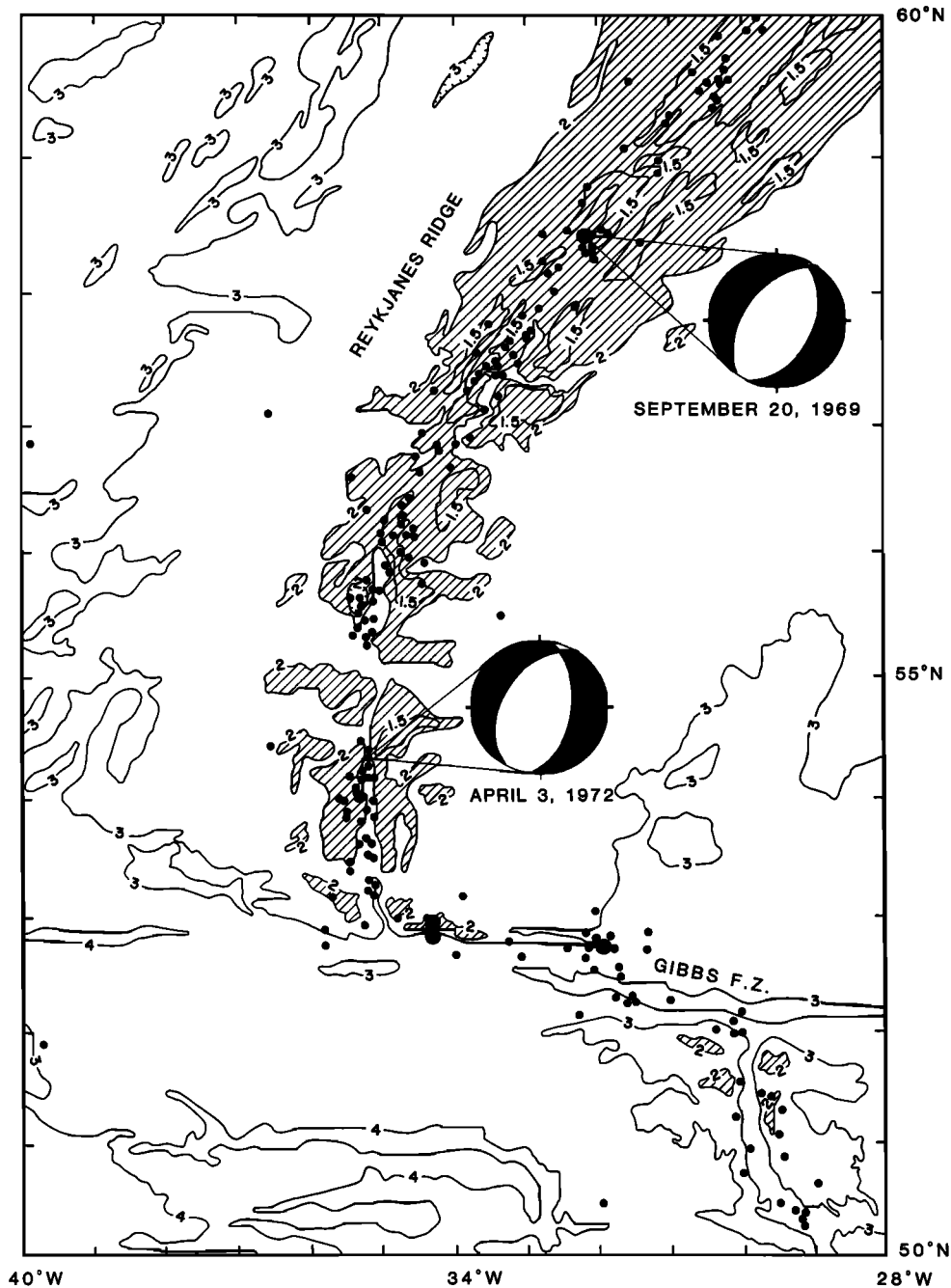


Fig. 10. Bathymetry and seismicity of the Reykjanes and Mid-Atlantic ridges near the epicenters of the earthquakes of September 20, 1969, and April 3, 1972. Bathymetric contours, in kilometers, are from *Laughton and Monahan [1978]*; regions shallower than 2 km are shaded. See Figure 6 for further explanation.

(0/45/255) with a seismic moment of 5×10^{24} dyn cm and a centroid depth of 1.5 km fits the observed *SH* waveforms for this earthquake quite well.

January 28, 1979

The January 28, 1979, earthquake occurred in the median valley near its intersection with a small fracture zone about 100 km north of the Vema Fracture Zone (Figure 6). The focal mechanism of this earthquake, as determined in the inversion, is pure normal faulting (20/46/270) with a seismic moment of 6.3×10^{24} dyn cm and a centroid depth of 2.2 km (Figure 18). The strike of the nodal planes differs by about 10° from the strike of the ridge axis. The *SH* waves are reasonably well fit,

but the station coverage for *SH* waves is inadequate to rule out a mechanism striking $N10^\circ E$ rather than $N20^\circ E$. The inferred water depth of 3.7 km is consistent with the epicenter shown in Figure 6.

April 22, 1979

The earthquake on April 22, 1979, occurred very near the epicenter of the June 6, 1972, event (Figure 8). Station coverage for both *P* and *SH* waves is excellent, and the observed waveforms are very well fit by a normal faulting mechanism (17/52/262), as shown in Figure 19. The centroid depth is 1.8 km and is very well constrained (Figure 2). The indicated water depth is 3.3 km, and the seismic moment is 9.9×10^{24}

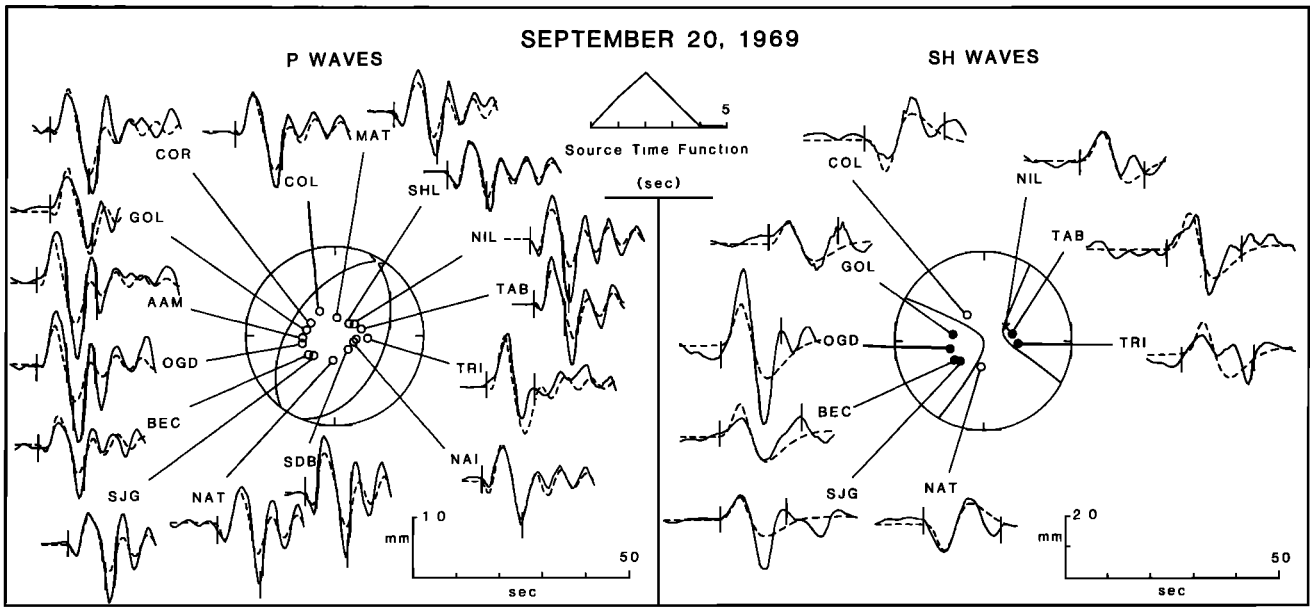


Fig. 11. Comparison of the observed and synthetic *P* and *SH* waves for the September 20, 1969, event. See Figure 5 for further explanation.

dyn cm. The double-couple orientation and both the centroid and water depths are very similar to those of the June 6, 1972, earthquake.

June 28, 1979

The June 28, 1979, earthquake occurred in the median valley about 30 km south of its eastern intersection with the St. Paul's Fracture Zone (Figure 20). Station coverage for

both *P* and *SH* waves is concentrated in the northern hemisphere. The focal mechanism of this event (Figure 21) is characterized by nearly pure normal faulting (346/40/280). The observed *P* and *SH* waves are well fit by this mechanism with a centroid depth of 2.5 km and a seismic moment of 3.6×10^{24} dyn cm. The inferred water depth is 3.5 km, consistent with the epicentral position and bathymetry shown in Figure 20.

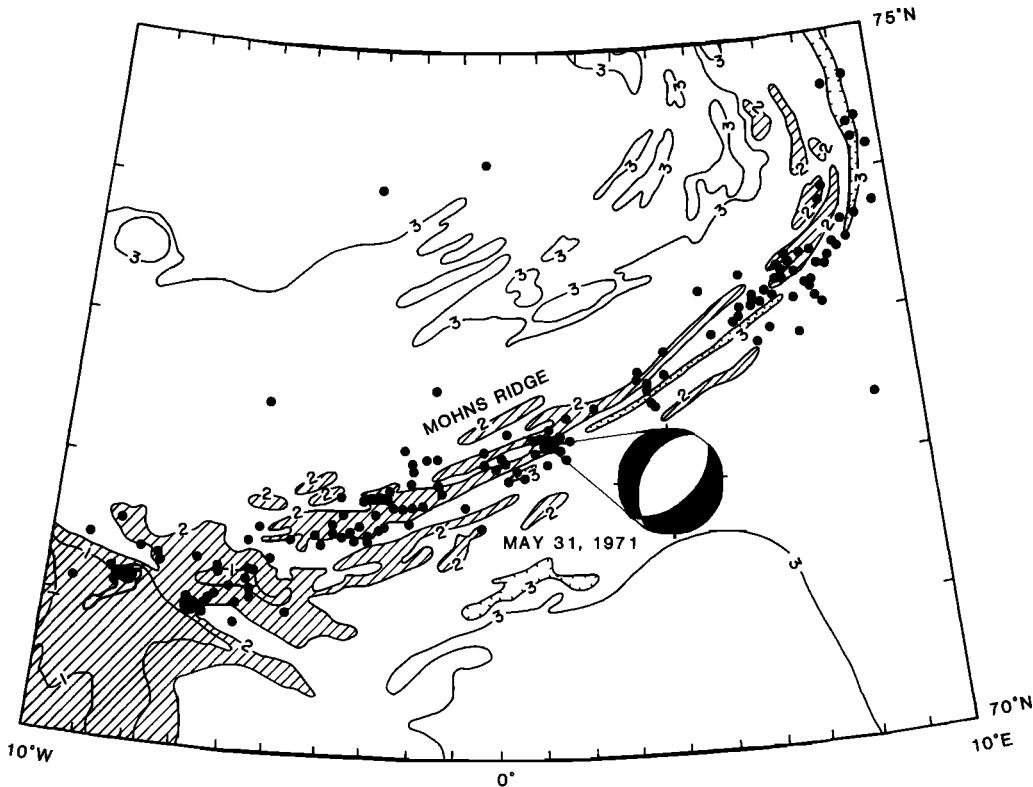


Fig. 12. Bathymetry and seismicity of the Mohns Ridge near the epicenter of the earthquake of May 31, 1971 (polar stereographic projection). Bathymetric contours, in kilometers, are from Johnson *et al.* [1979]; regions shallower than 2 km are shaded. See Figure 6 for further explanation.

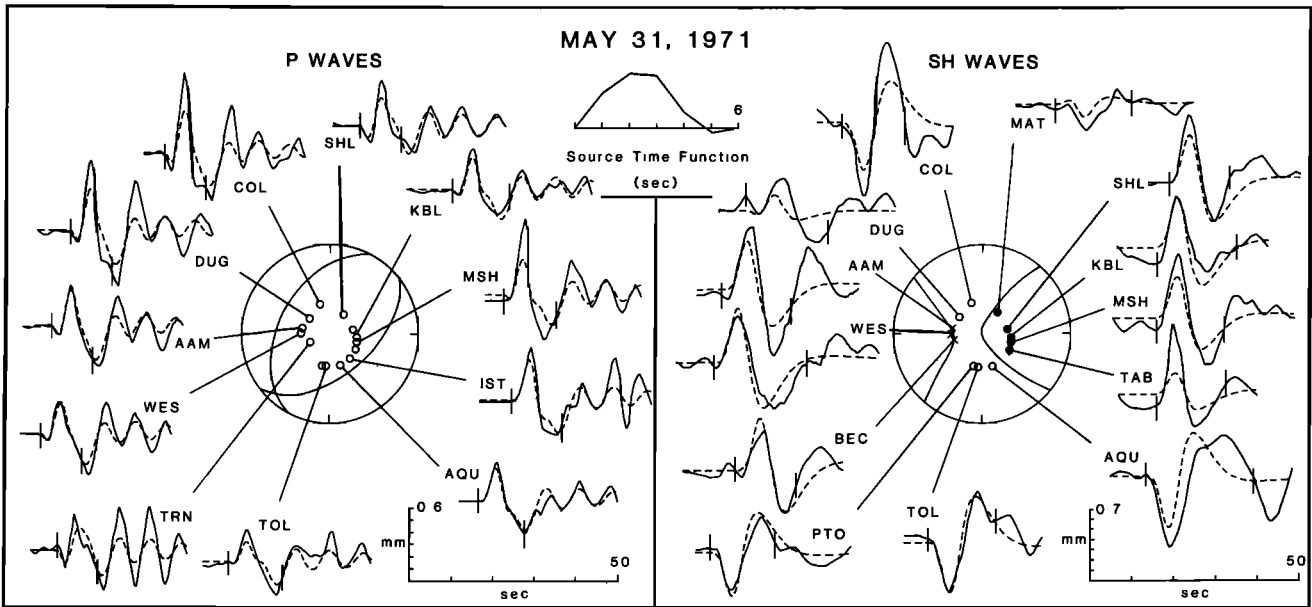


Fig. 13. Comparison of the observed and synthetic *P* and *SH* waves for the May 31, 1971, event. See Figure 5 for further explanation.

January 29, 1982

The January 29, 1982, earthquake occurred in the median valley about 200 km north of the Kane Fracture Zone (Figure 22). Using a semiautomated centroid moment tensor inversion and data from the GDSN, *Dziewonski et al.* [1983a] obtained a normal faulting mechanism with a significant strike-slip component (353/61/246). Station coverage, particularly for *P* waves, is rather poor for this event because many records have not yet been distributed. From the body waveform inversion, we obtained a nearly pure normal-faulting mechanism (9/44/264) with fault planes striking subparallel to the local trend of the ridge axis (Figure 23). Most of the waveforms are well fit by the synthetic seismograms, especially the nodal character of the *SH* wave at KBS. The seismic moment of

5.4×10^{24} dyn cm is somewhat smaller than the 8.1×10^{24} dyn cm obtained by *Dziewonski et al.* [1983a]. The centroid depth is 2.4 km, and the water depth 3.8 km.

May 12, 1983

The earthquake of May 12, 1983, occurred in the median valley about 250 km north of the 15°20' Fracture Zone (Figure 6). A centroid moment tensor solution (354/50/259) by *Dziewonski et al.* [1983b] shows predominantly normal faulting motion. Station coverage for this event is good, and the focal mechanism is well resolved. Our inversion solution (341/48/251) shown in Figure 24 is very similar to that of *Dziewonski* and coworkers. One of the nodal planes is subparallel to the local trend of the ridge axis. The seismic

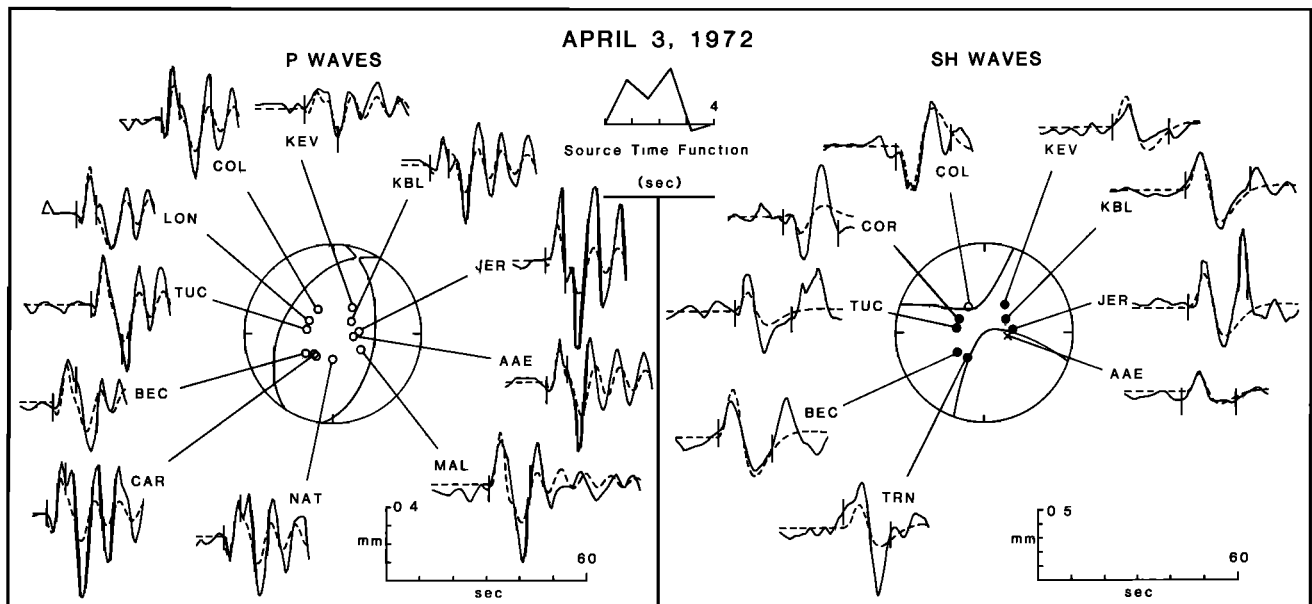


Fig. 14. Comparison of the observed and synthetic *P* and *SH* waves for the April 3, 1972, event. See Figure 5 for further explanation.

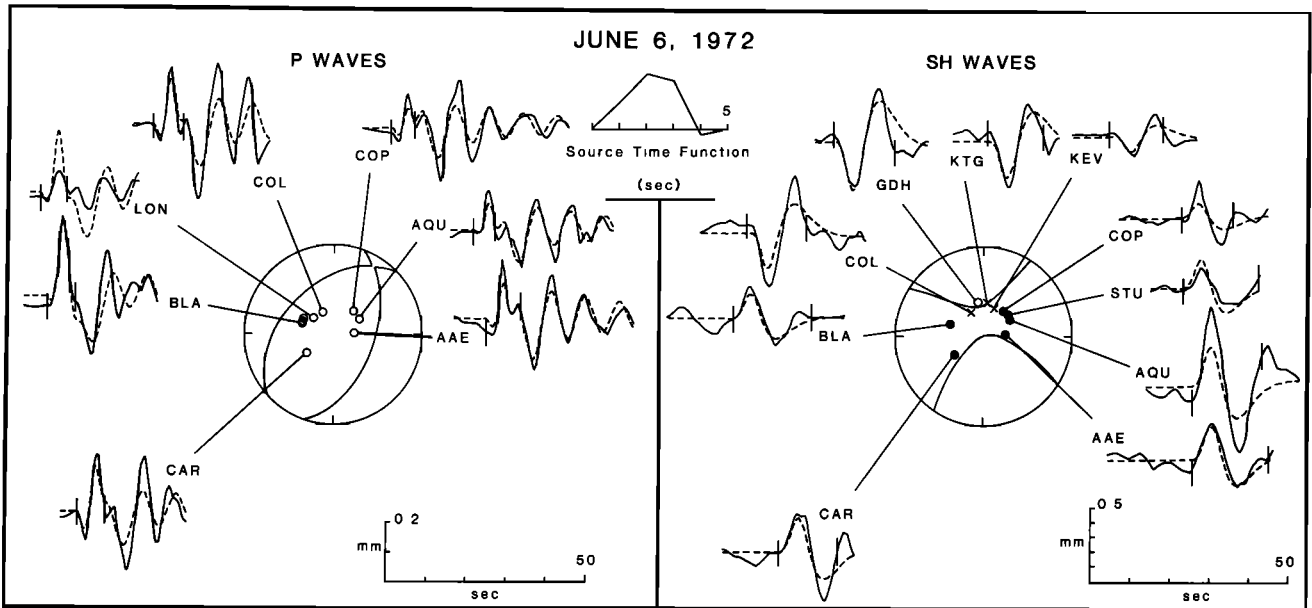


Fig. 15. Comparison of the observed and synthetic *P* and *SH* waves for the June 6, 1972, event. See Figure 5 for further explanation.

moment of 7.1×10^{24} dyn cm is similar to the 8.1×10^{24} dyn cm obtained by Dziewonski *et al.* [1983b]. The centroid depth is 3.1 km, and the inferred water depth is 4.1 km.

DISCUSSION

The 14 earthquakes of this study are remarkably similar in their source characteristics. All show normal-faulting mechanisms with at least one nodal plane dipping at about 45° and striking approximately parallel to the local trend of the ridge axis. The inferred *T* axes are all nearly horizontal and are approximately aligned with the spreading direction. The seismic moments span a range of only a factor of 5, from 3 to 15×10^{24} dyn cm, and the source time functions are of generally similar duration. The centroid depths are all very shallow, between 1.2 and 3.1 km beneath the seafloor.

The water depth at the epicenter of each of these earthquakes is well constrained by the predominant period of the large water column reverberations in the *P* wave trains. The water depth estimated from the *P* waveform is compared in Table 1 with the maximum local depth of the median valley as indicated on available bathymetric maps. Given the uncertainties in the epicentral coordinates and in the depths obtained from contour maps constructed from ship track data of variable sampling density and accuracy, the agreement between the two depth estimates is surprisingly good, to within a few hundred meters for all earthquakes in Table 1. We conclude from this comparison that all of the earthquakes in this study occurred beneath the inner floor of the median valley. We cannot exclude the possibility that some of these events occurred near the inner walls of the rift valley (e.g., the May

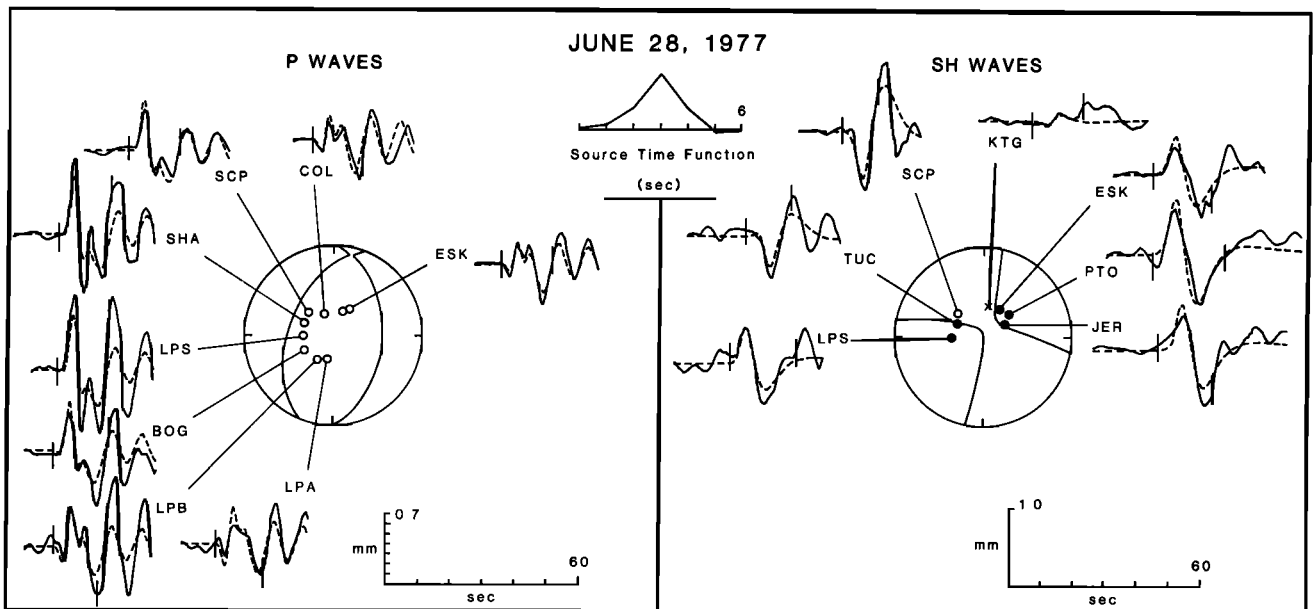


Fig. 16. Comparison of the observed and synthetic *P* and *SH* waves for the $m_b = 5.9$ event of June 28, 1977. See Figure 5 for further explanation.

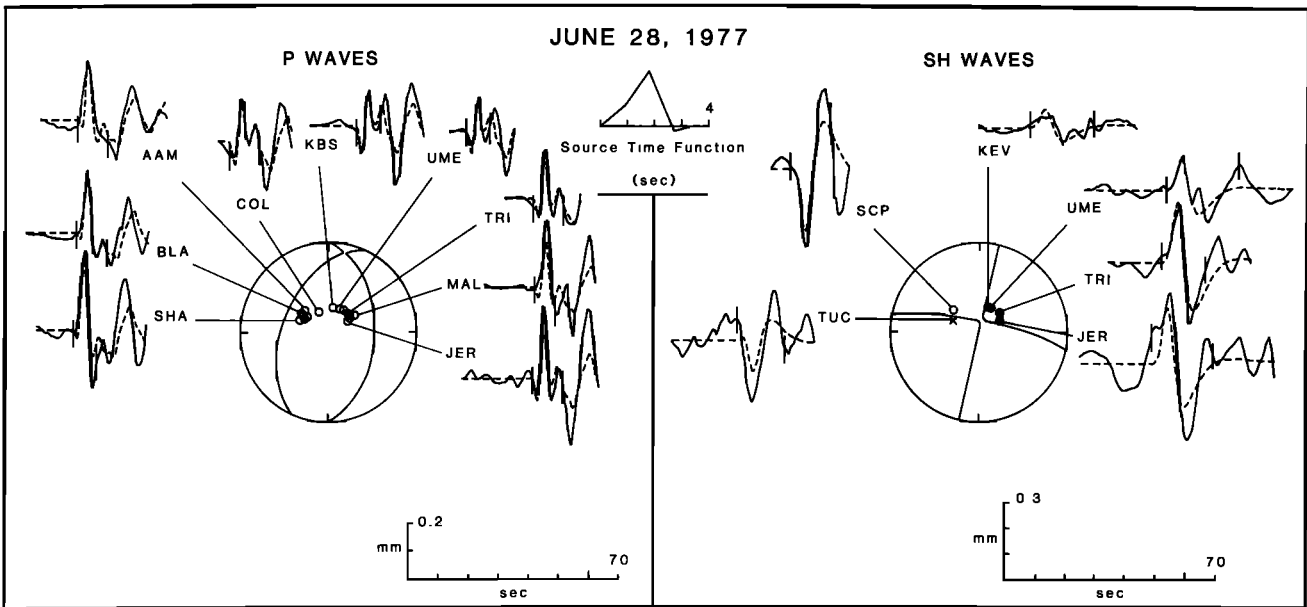


Fig. 17. Comparison of the observed and synthetic *P* and *SH* waves for the $m_b = 5.3$ event of June 28, 1977. This earthquake was the first in a series of five events within 4 hours, including the earthquake of Figure 16. See Figure 5 for further explanation.

31, 1971, earthquake) or that they represent slip on major inward dipping faults that contribute to the relief of the inner valley walls [Macdonald and Luyendyk, 1977]. It may be inferred with reasonable certainty, however, that none of the Mid-Atlantic Ridge earthquakes in Table 1 occurred beneath the rift mountains.

Perhaps the most important result of this work is that all 14 earthquakes studied have centroid depths less than or equal to 3 km beneath the seafloor. On the basis of the numerical experiments and statistical tests described earlier, these centroid depths are estimated to have uncertainties of ± 2 km for the smaller events and somewhat lesser uncertainties for the larger events. In the interpretation of these centroid depths, it is important to note that the centroid depth does not mark the maximum depth of fault slip. If the fault is rectangular or

circular in shape and the slip is approximately uniform, then the centroid should lie near the geometric center of the fault. Since prominent water column reverberations are evident in the *P* waves from these events, it is reasonable to infer that fault rupture extends to the seafloor. Under these conditions, the maximum depth of fault slip is twice the centroid depth, or 2–6 km below the seafloor for the earthquakes of this study. Given the uncertainty in centroid depth and the possibility of irregular fault shape or nonuniform slip, however, the maximum depth of fault slip may have exceeded 6 km for some of these events.

Two microearthquake experiments conducted with a sufficient number of ocean bottom sensors to resolve focal depths [Francis et al., 1978; Toomey et al., 1985] were conducted in regions of the Mid-Atlantic Ridge near epicenters of one or

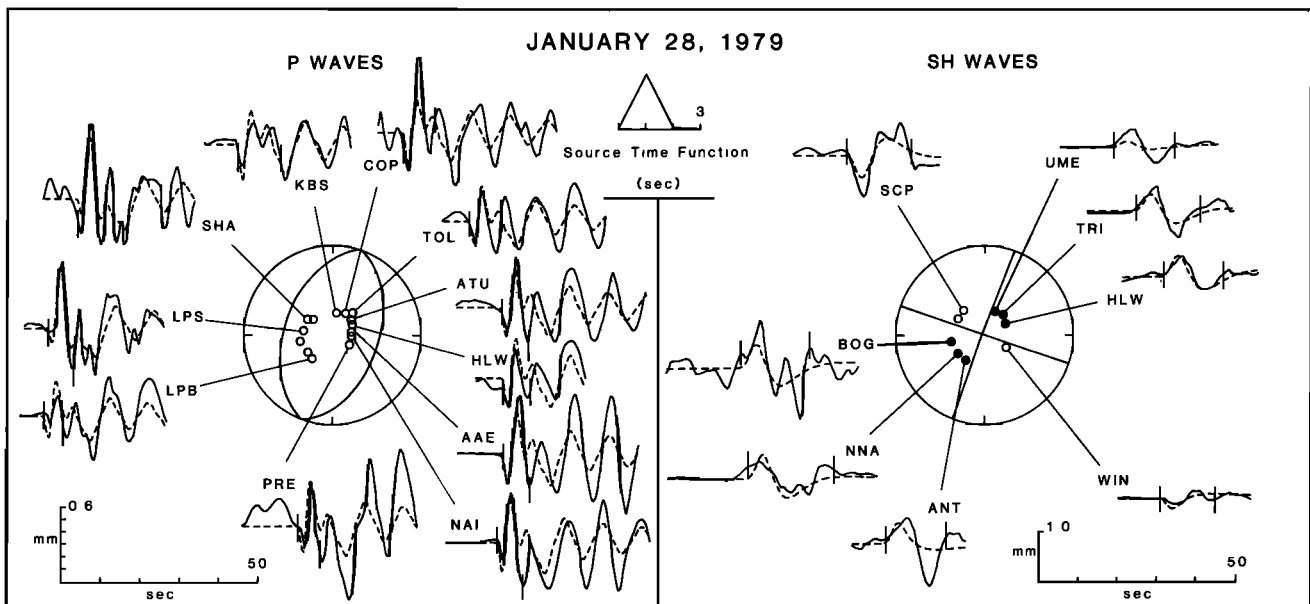


Fig. 18. Comparison of the observed and synthetic *P* and *SH* waves for the January 28, 1979, event. See Figure 5 for further explanation.

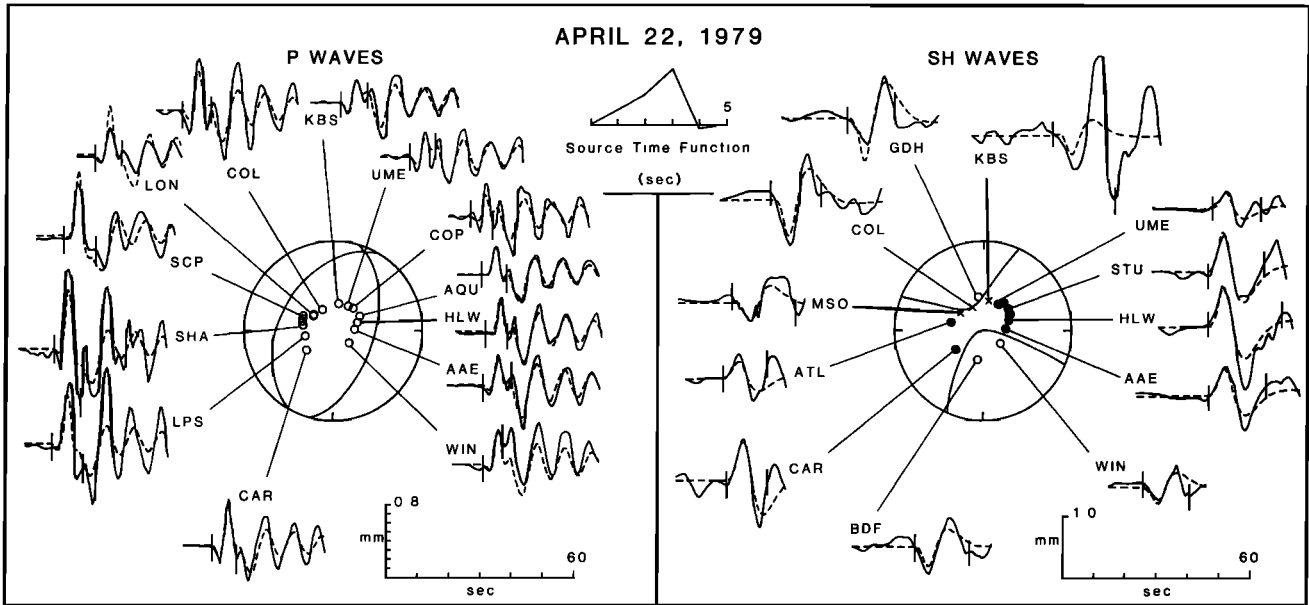


Fig. 19. Comparison of the observed and synthetic *P* and *SH* waves for the April 22, 1979, event. See Figure 5 for further explanation.

more of the large earthquakes of this study. It is of interest to compare the distribution of microearthquake focal depths with the centroid depths obtained for the large earthquakes.

Francis *et al.* [1978] reported the locations of a number of microearthquakes recorded during December 1974 by a network of four ocean bottom seismometers near the eastern intersection of the St. Paul's Fracture Zone and the Mid-Atlantic Ridge median valley. Focal depths concentrated in

the ranges 0–1 km and 6–8 km. Francis *et al.* [1978] commented particularly on the absence of median valley events with focal depths between 1 and 5 km, which they attributed to the presence of an intracrustal layer highly cracked and weakened by pervasive hydrothermal circulation. The earthquake of June 28, 1979 (Figure 20), occurred beneath the median valley at the southern end of the zone of microearthquakes described by Francis *et al.* [1978]. The centroid depth of 2.5 km and the

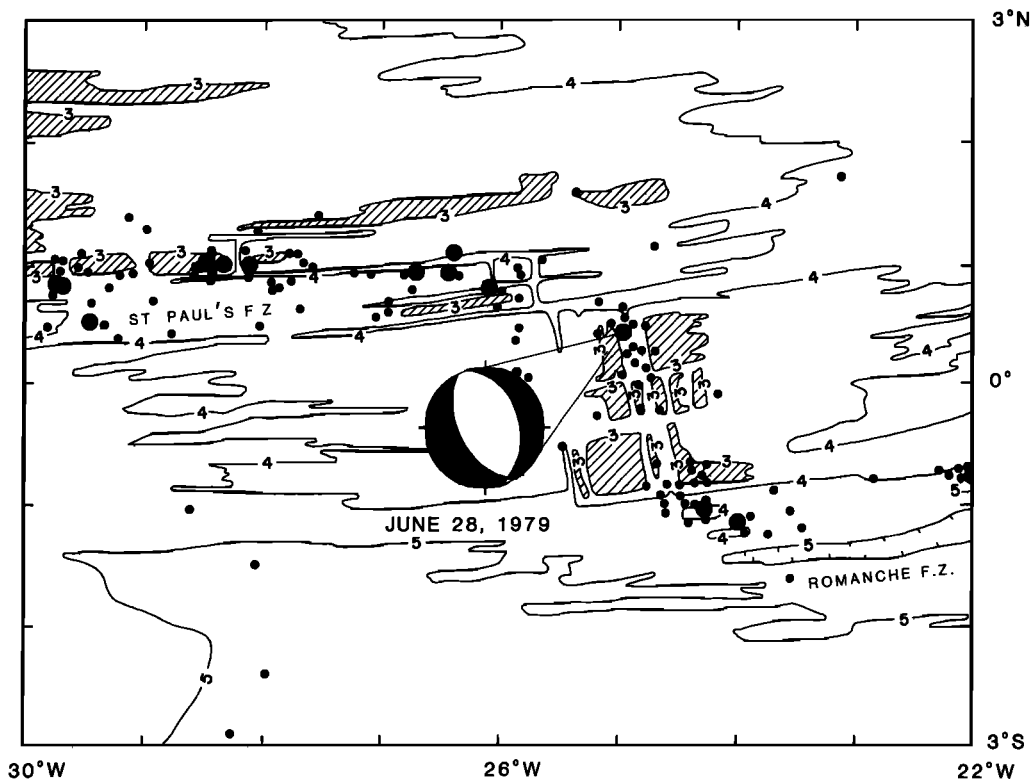


Fig. 20. Bathymetry and seismicity of the Mid-Atlantic Ridge near the epicenter of the earthquake of June 28, 1979. Bathymetric contours, in kilometers, are from Heezen and Tharp [1978]; regions shallower than 3 km are shaded. See Figure 6 for further explanation.

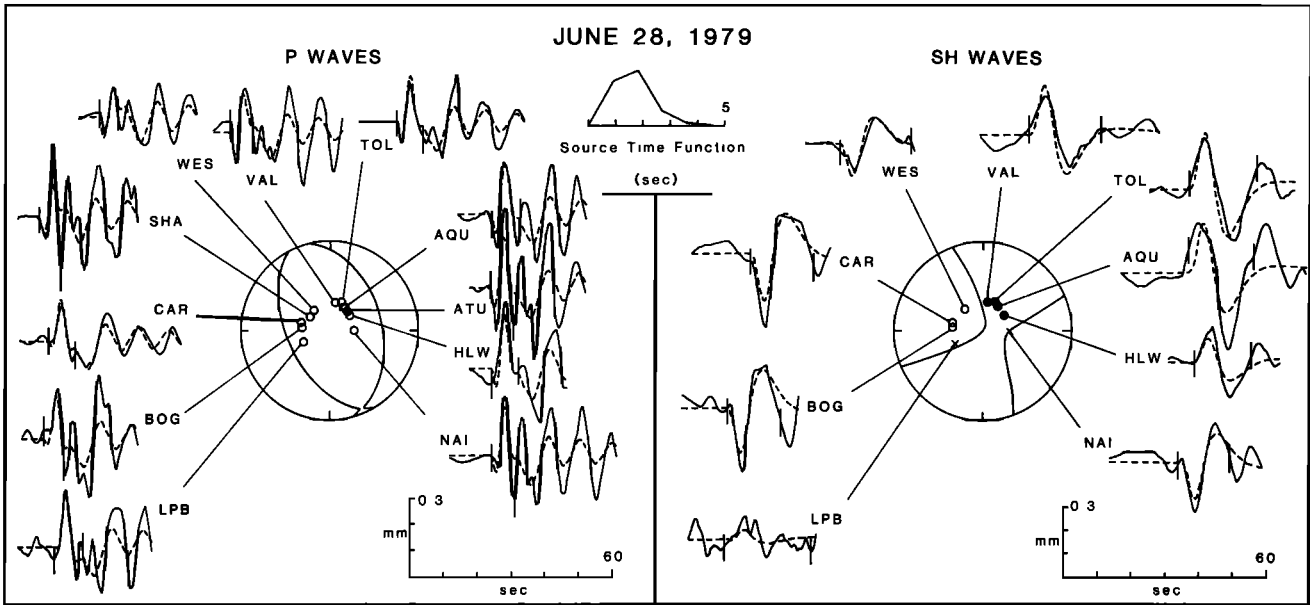


Fig. 21. Comparison of the observed and synthetic *P* and *SH* waves for the June 28, 1979, event. See Figure 5 for further explanation.

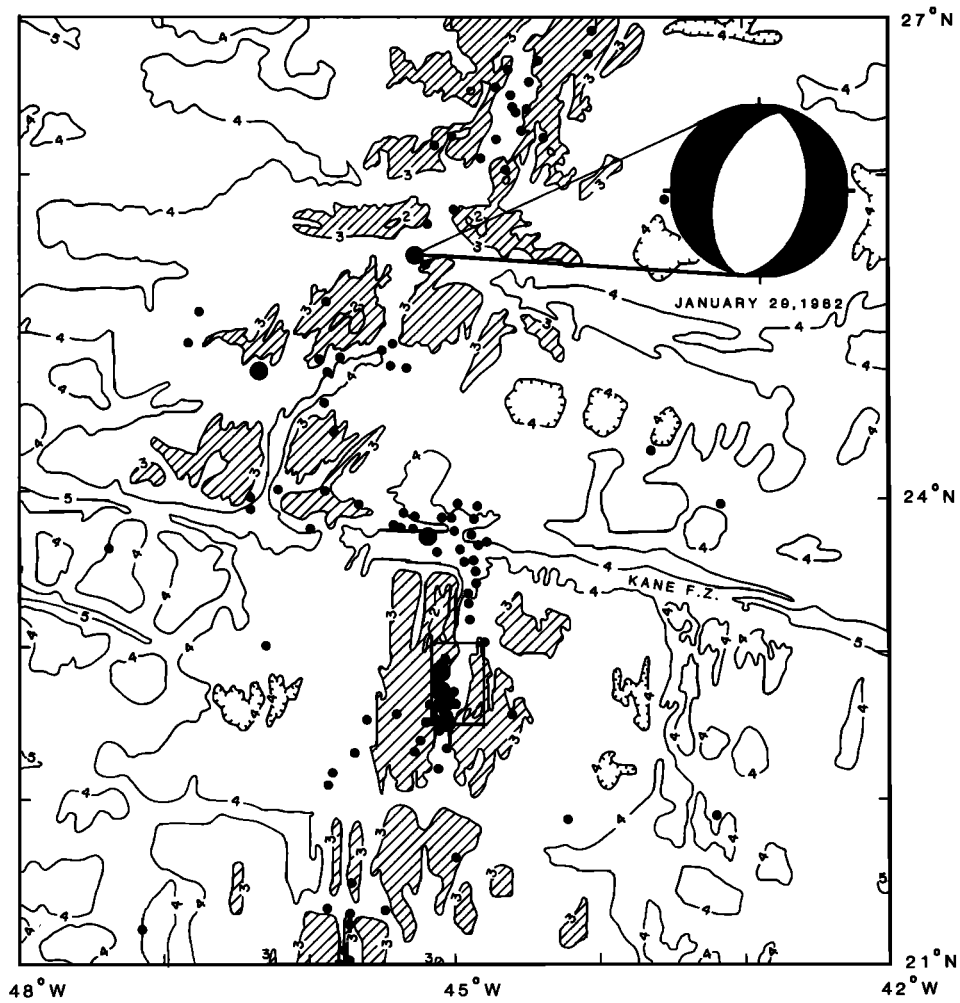


Fig. 22. Bathymetry and seismicity of the Mid-Atlantic Ridge near the epicenter of the earthquake of January 29, 1982. Bathymetric contours, in kilometers, are from *Searle et al.* [1982]; regions shallower than 3 km are shaded. The small box centered on the median valley near 23°N outlines the area shown in greater detail in Figure 4. See Figure 6 for further explanation.

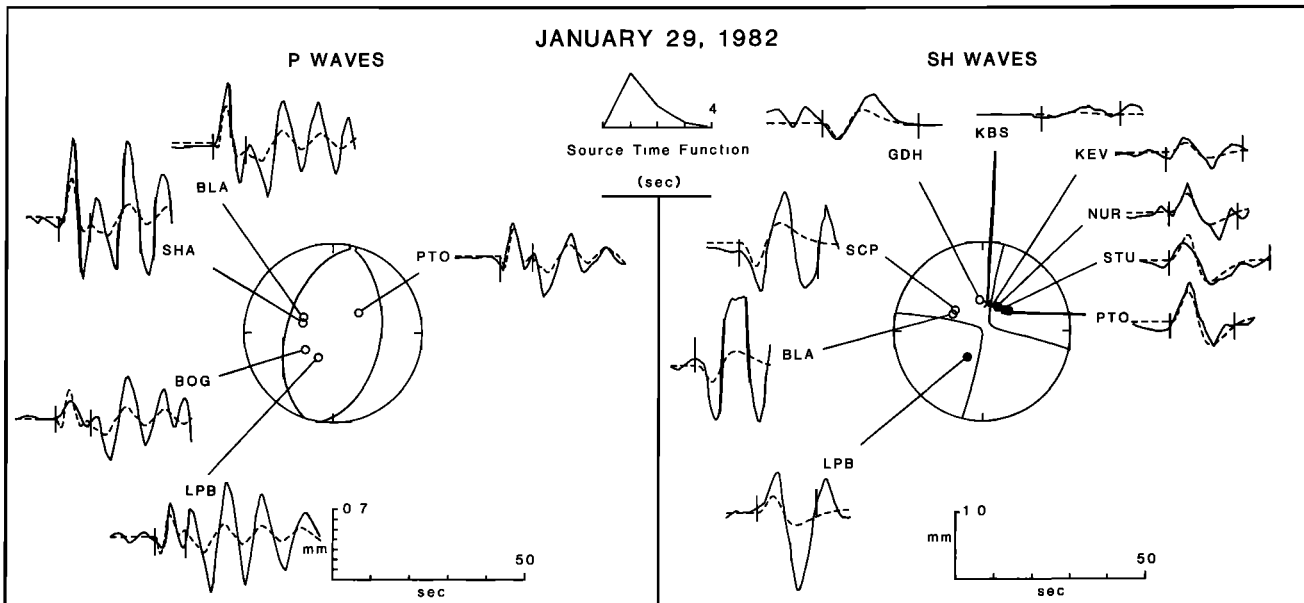


Fig. 23. Comparison of the observed and synthetic *P* and *SH* waves for the January 29, 1982, event. See Figure 5 for further explanation.

large water column reverberations shown in the *P* waveforms (Figure 21), if taken at face value, would indicate that seismic slip was concentrated between the seafloor and 5 km depth. If correct, this result suggests that the microearthquakes in 1974 may have outlined the top and bottom of the slip zone of the large earthquake that followed 4.5 years later. Of course, the uncertainties in both the centroid depth and the microearthquake focal depths also permit a coincidence in depth of the two measures of activity.

The second microearthquake experiment was conducted early in 1982 in the Mid-Atlantic Ridge median valley near 23°N, approximately 90 km south of the Kane Fracture Zone [Toomey *et al.*, 1985]. Because of the large network (10 stations) and knowledge of the local crustal velocity structure [Purdy and Detrick, 1986], the focal depths of many of the microearthquakes were determined to within ± 1 km formal error at 95% confidence. Most of the well-resolved hypocenters were located between 5 and 8 km beneath the seafloor. Three large earthquakes of our study occurred in the same region in 1962 and 1977 (Figure 4). Their fault plane solutions are quite similar to composite fault plane solutions obtained for two clusters of microearthquakes [Toomey *et al.*, 1985], indicating that both sets of events are probably responding to the same tectonic process. The centroid depths of the large earthquakes are 1.2–2.5 km, values most readily interpreted as indicating that slip extended between the seafloor and about 5 km depth. Most of the 1982 microearthquakes thus occurred deeper than this nominal slip zone of the large earthquakes 5 and 20 years earlier, but the uncertainties in both sets of quantities also permit the large earthquake slip zones to have extended well into the depth range of microearthquake activity.

If the difference in depth between the slip zones of the large earthquakes and the regions of most intense microearthquake activity along these two segments of the Mid-Atlantic Ridge is real, then two possible explanations present themselves. One possibility is that microearthquakes in the median valley outline a strong portion of the crust [Kanamori, 1981] between 1–2 and 5–6 km depth and that fault rupture during large earthquakes initiates near the base of the crust and propagates upward to the seafloor. If a large proportion of fault area or

slip were concentrated in the upper crust for these large events, the depth of the centroid would be shallower than half the maximum depth of fault slip. According to this scenario, the microearthquake focal depths provide the most accurate measure of the maximum depth of brittle behavior. A second possibility is based on the premise that the microearthquake at 5–8 km depth mark the strongest portion of the median valley faults. In this scenario, the strong zone acts as a barrier [Aki, 1979] to the downward propagation of fault slip during the large earthquakes of this study. Continued microearthquake activity is the result of the large stress differences remaining near the base of the slip zone of the larger events. This scenario admits the possibility of a rare, very large ridge axis earthquake that breaks through the barrier and has a significantly greater centroid depth and moment than any of the events of this study. While we favor the first scenario, we are unable to exclude the second one. Possible avenues of research to distinguish between them include searching for directivity effects in short-period waveforms, monitoring aftershocks shortly following a large event, and discovering an unusually large ($M_0 \gtrsim 10^{26}$ dyn cm) normal-faulting earthquake along an ocean ridge segment.

The source properties listed in Table 1 offer an opportunity to look for interrelationships among parameters for an unusually homogeneous set of earthquakes. We tested for systematic variations of centroid depth, for instance, with local spreading rate [Minster and Jordan, 1978]; no relationship is resolvable. We also tested for a relationship between centroid depth and seismic moment; for the events in Table 1 these quantities show no significant correlation.

From the centroid depth, the source time function, and the seismic moment, we can obtain rough estimates of fault dimensions, average slip, and average stress drop for these earthquakes. For simplicity, we assume that the zone of slip is rectangular, with horizontal length L and downdip width w . We estimate L from the length t_s of the source time function. On the basis of the large water column reverberations we assume that rupture extended to the surface, and we estimate w from the centroid depth. For unilateral rupture $L = V_r t_s$, where the rupture velocity V_r is taken to be equal to 0.9 times

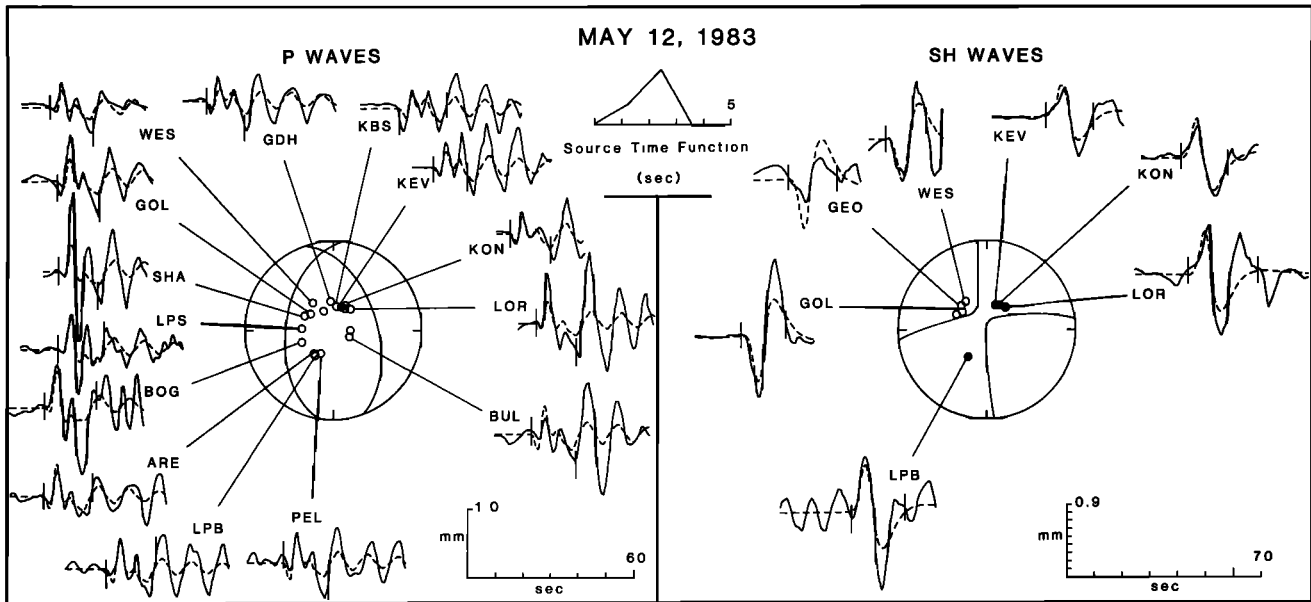


Fig. 24. Comparison of the observed and synthetic P and SH waves for the May 12, 1983, event. See Figure 5 for further explanation.

the shear velocity, or 3.3 km/s. We estimate w from $w = 2.8h$, where h is the centroid depth; this relation follows from a fault dip of about 45° and a centroid depth that marks the average depth of fault slip. The average slip D can be estimated from the relation $M_0 = \mu LwD$ [Aki, 1966], where the rigidity μ of the crust is taken to be 4.0×10^{11} dyn/cm² from our assumed crustal structure. The stress drop $\Delta\sigma$ can be estimated from the relation $\Delta\sigma = cM_0/(Lw^2)$, where c is a geometrical constant near unity [Knopoff, 1958; Aki, 1966].

The estimated fault area Lw ranges from 30 to 110 km² and shows no resolvable correlation with moment for the limited set of events studied here. The average fault slip varies from 10 to 70 cm. The estimated stress drops lie between 10 and 60 bars, within the range shown by other tectonic earthquakes [Kanamori and Anderson, 1975].

CONCLUSIONS

We have determined the source mechanisms and centroid depths of 14 earthquakes on the Mid-Atlantic Ridge from an inversion of long-period P and SH waveforms. All events have mechanisms characterized dominantly by normal faulting on fault planes with dip angles near 45° . Moments range from 3 to 15×10^{24} dyn cm, and the source time functions are all of simple form. The water depths estimated from the predominant period of water column reverberations in the P wave trains indicate that the earthquakes in this study all occurred beneath the inner floor of the median valley. The centroid depths of these earthquakes are all very shallow, ranging from 1 to 3 km. If the centroid depth marks the mean depth of fault slip, then earthquake faulting extended up to 6 km beneath the seafloor during these events. A limited amount of slip at somewhat greater depths cannot be excluded.

This study raises several issues concerning the tectonic interpretation of ridge crest earthquakes, including the relationship of microearthquakes and large earthquakes along a given ridge axis segment, the relationship of earthquake activity within the inner median valley to fault structures in the adjacent rift mountains, and possible variations of source properties with spreading rate or other parameters. To address these

issues will require extensions of this study to additional events, other regions, and an expanded frequency band.

Acknowledgments. We thank Doug Toomey for helpful discussions, Emile Okal and Lisa Stewart for comments on an early draft, and Jan Nattier-Barbaro for assistance in manuscript preparation. This research was supported by the National Science Foundation under grants EAR-8115908 and EAR-8416192.

REFERENCES

- Aki, K., Generation and propagation of G waves from the Niigata earthquake of June 16, 1964, part 2, Estimation of earthquake moment, released energy, and stress-strain drop from the G wave spectrum, *Bull. Earthquake Res. Inst. Univ. Tokyo*, **44**, 73–88, 1966.
- Aki, K., Characterization of barriers on an earthquake fault, *J. Geophys. Res.*, **84**, 6140–6148, 1979.
- Aki, K., and H. Patton, Determination of seismic moment tensor using surface waves, *Tectonophysics*, **43**, 213–222, 1978.
- Aki, K., and P. G. Richards, *Quantitative Seismology: Theory and Methods*, vol. 1, p. 114, W. H. Freeman, San Francisco, Calif., 1980.
- Bergman, E. A., and S. C. Solomon, Source mechanisms of earthquakes near mid-ocean ridges from body waveform inversion: Implications for the early evolution of oceanic lithosphere, *J. Geophys. Res.*, **89**, 11415–11441, 1984.
- Bergman, E. A., and S. C. Solomon, Earthquake source mechanisms from body-waveform inversion and intraplate tectonics in the northern Indian Ocean, *Phys. Earth Planet. Inter.*, **40**, 1–23, 1985a.
- Bergman, E. A., and S. C. Solomon, Broad-band and short-period body waveform inversion for source characterization of ridge-crest earthquakes (abstract), *Eos Trans. AGU*, **66**, 355, 1985b.
- Bergman, E. A., J. L. Nabelek, and S. C. Solomon, An extensive region of off-ridge normal-faulting earthquakes in the southern Indian Ocean, *J. Geophys. Res.*, **89**, 2425–2443, 1984.
- Bunch, A. W. H., and B. L. N. Kennett, The crustal structure of the Reykjanes Ridge at $59^\circ 30'N$, *Geophys. J. R. Astron. Soc.*, **61**, 141–166, 1980.
- Conant, D. A., Six new focal mechanism solutions for the Arctic and a center of rotation for plate movements, M.A. thesis, 18 pp., Columbia Univ., New York, 1972.
- Duschesnes, J. D., and S. C. Solomon, Shear wave travel time residuals from oceanic earthquakes and the evolution of oceanic lithosphere, *J. Geophys. Res.*, **82**, 1985–2000, 1977.
- Duschesnes, J., R. C. Lilwall, and T. J. G. Francis, The hypocentral resolution of microearthquake surveys carried out at sea, *Geophys. J. R. Astron. Soc.*, **72**, 435–451, 1983.
- Dziewonski, A. M., A. Friedman, D. Giardini, and J. H. Woodhouse,

- Global seismicity of 1982: Centroid-moment tensor solutions for 308 earthquakes, *Phys. Earth Planet. Inter.*, **33**, 76–90, 1983a.
- Dziewonski, A. M., J. E. Franzen, and J. H. Woodhouse, Centroid-moment tensor solutions for April–June 1983, *Phys. Earth Planet. Inter.*, **33**, 243–249, 1983b.
- Einarsson, P., Seismicity and earthquake focal mechanisms along the mid-Atlantic plate boundary between Iceland and the Azores, *Tectonophysics*, **55**, 127–153, 1979.
- Fowler, C. M. R., Crustal structure of the Mid-Atlantic Ridge at 37°N, *Geophys. J. R. Astron. Soc.*, **47**, 459–491, 1976.
- Francis, T. J. G., The seismicity of the Reykjanes Ridge, *Earth Planet. Sci. Lett.*, **18**, 119–124, 1973.
- Francis, T. J. G., I. T. Porter and R. C. Lilwall, Microearthquakes near the eastern end of St. Paul's Fracture Zone, *Geophys. J. R. Astron. Soc.*, **53**, 201–217, 1978.
- Futterman, W. I., Dispersive body waves, *J. Geophys. Res.*, **67**, 5279–5291, 1962.
- Hart, R. S., Body wave studies of the September 20, 1969, North Atlantic Ridge earthquake (abstract), *Eos Trans. AGU*, **59**, 1135, 1978.
- Heezen, B. C., and M. Tharp, General bathymetric chart of the oceans (GEBCO), 5th ed., sheet 5.12, Can. Hydrogr. Serv., Ottawa, 1978.
- Isacks, B., J. Oliver, and L. R. Sykes, Seismology and the new global tectonics, *J. Geophys. Res.*, **73**, 5855–5899, 1968.
- Jemsek, J. P., E. A. Bergman, J. L. Nabelek, and S. C. Solomon, Focal depths and mechanisms of large earthquakes on the Mid-Arctic Ridge system (abstract), *Eos Trans. AGU*, **65**, 273, 1984.
- Johnson, G. L., D. Monahan, G. Grönlie, and L. Sobczak, General bathymetric chart of the oceans (GEBCO), 5th ed., sheet 5.17, Can. Hydrogr. Serv., Ottawa, 1979.
- Kanamori, H., The nature of seismicity patterns before large earthquakes, in *Earthquake Prediction: An International Review*, Maurice Ewing Ser., vol. 4, edited by D. W. Simpson and P. G. Richards, pp. 1–19, AGU, Washington, D. C., 1981.
- Kanamori, H., and D. L. Anderson, Theoretical basis of some empirical relations in seismology, *Bull. Seismol. Soc. Am.*, **65**, 1073–1095, 1975.
- Knopoff, L., Energy release in earthquakes, *Geophys. J. R. Astron. Soc.*, **1**, 44–52, 1958.
- Laughton, A. S., and D. Monahan, General bathymetric chart of the oceans (GEBCO), 5th ed., sheet 5.04, Can. Hydrogr. Serv., Ottawa, 1978.
- Lister, C. R. B., Qualitative models of spreading-center processes, including hydrothermal penetration, *Tectonophysics*, **37**, 203–218, 1977.
- Macdonald, K. C., and B. P. Luyendyk, Deep-tow studies of the studies of the structure of the Mid-Atlantic Ridge crest near lat 37°N, *Geol. Soc. Am. Bull.*, **88**, 621–636, 1977.
- Minster, J. B., and T. H. Jordan, Present-day plate motions, *J. Geophys. Res.*, **83**, 5331–5354, 1978.
- Nabelek, J. L., Determination of earthquake source parameters from inversion of body waves, Ph.D. thesis, 346 pp., Mass. Inst. of Technol., Cambridge, 1984.
- Pearce, R. G., Complex *P* waveforms from a Gulf of Aden earthquake, *Geophys. J. R. Astron. Soc.*, **64**, 187–200, 1981.
- Purdy, G. M., and R. S. Detrick, The crustal structure of the Mid-Atlantic Ridge at 23°N from seismic refraction studies, *J. Geophys. Res.*, in press, 1986.
- Romanowicz, B., Depth resolution of earthquakes in central Asia by moment tensor inversion of long period Rayleigh waves: Effects of phase velocity variations across Eurasia and their calibrations, *J. Geophys. Res.*, **86**, 5963–5984, 1981.
- Romanowicz, B. A., Moment tensor inversion of long-period Rayleigh waves: A new approach, *J. Geophys. Res.*, **87**, 5395–5407, 1982.
- Rothé, J. P., *The Seismicity of the Earth*, 336 pp., UNESCO, Paris, 1969.
- Savostin, L. A., and A. M. Karasik, Recent plate tectonics of the Arctic Basin and of northeastern Asia, *Tectonophysics*, **74**, 111–145, 1981.
- Searle, R. C., D. Monahan, and G. L. Johnson, General bathymetric chart of the oceans (GEBCO), 5th ed., sheet 5.08, Can. Hydrogr. Serv., Ottawa, 1982.
- Solomon, S. C., and B. R. Julian, Seismic constraints on ocean-ridge mantle structure: Anomalous fault-plane solutions for first motions, *Geophys. J. R. Astron. Soc.*, **38**, 265–285, 1974.
- Sykes, L. R., Mechanism of earthquakes and nature of faulting on the mid-oceanic ridges, *J. Geophys. Res.*, **72**, 2131–2153, 1967.
- Sykes, L. R., Focal mechanism solutions for earthquakes along the world rift system, *Bull. Seismol. Soc. Am.*, **60**, 1749–1752, 1970.
- Tarr, A. C., World seismicity map, U. S. Geol. Surv., Reston, Va., 1974.
- Thatcher, W., and J. N. Brune, Seismic study of an oceanic ridge earthquake swarm in the Gulf of California, *Geophys. J. R. Astron. Soc.*, **22**, 473–489, 1971.
- Toomey, D. R., S. C. Solomon, G. M. Purdy, and M. H. Murray, Microearthquakes beneath the median valley of the Mid-Atlantic Ridge near 23°N: Hypocenters and focal mechanisms, *J. Geophys. Res.*, **90**, 5443–5458, 1985.
- Tréhu, A. M., J. L. Nabelek, and S. C. Solomon, Source characterization of two Reykjanes Ridge earthquakes: Surface waves and moment tensors; *P* waveforms and nonorthogonal nodal planes, *J. Geophys. Res.*, **86**, 1701–1724, 1981.
- Tsai, Y. B., Determination of focal depths of earthquakes in mid-oceanic ridges from amplitude spectra of surface waves, Ph.D. thesis, 144 pp., Mass. Inst. of Technol., Cambridge, 1969.
- Udías, A., A. López Arroyo, and J. Mezcua, Seismotectonics of the Azores-Alboran region, *Tectonophysics*, **31**, 259–289, 1976.
- Vogt, P., and G. L. Johnson, Transform faults and longitudinal flow below the mid-oceanic ridge, *J. Geophys. Res.*, **80**, 1399–1428, 1975.
- Weidner, D. J., and K. Aki, Focal depth and mechanism of mid-ocean ridge earthquakes, *J. Geophys. Res.*, **78**, 1818–1831, 1973.

E. A. Bergman, P. Y. Huang, J. L. Nabelek, and S. C. Solomon, Department of Earth, Atmospheric, and Planetary Sciences, Massachusetts Institute of Technology, Cambridge, MA 02139.

(Received February 22, 1985;
revised September 18, 1985;
accepted September 20, 1985.)